The Plant Cell, Vol. 22: 273–292, January 2010, www.plantcell.org © 2010 American Society of Plant Biologists

Jasmonate and ppHsystemin Regulate Key Malonylation Steps in the Biosynthesis of 17-Hydroxygeranyllinalool Diterpene Glycosides, an Abundant and Effective Direct Defense against Herbivores in *Nicotiana attenuata* [W]

Sven Heiling,[a,1] Meredith C. Schuman,[a,1] Matthias Schoettner,[a] Purba Mukerjee,[a,2] Beatrice Berger,[a,3] Bernd Schneider,[b] Amir R. Jassbi,[a,4] and Ian T. Baldwin[a,5]

[a] Department of Molecular Ecology, Max Planck Institute for Chemical Ecology, Jena, Germany 07745
[b] Department of Biosynthesis/Nuclear Magnetic Resonance, Max Planck Institute for Chemical Ecology, Jena, Germany 07745

We identified 11 17-hydroxygeranyllinalool diterpene glycosides (HGL-DTGs) that occur in concentrations equivalent to starch (mg/g fresh mass) in aboveground tissues of coyote tobacco (*Nicotiana attenuata*) and differ in their sugar moieties and malonyl sugar esters (0-2). Concentrations of HGL-DTGs, particularly malonylated compounds, are highest in young and reproductive tissues. Within a tissue, herbivore elicitation changes concentrations and biosynthetic kinetics of individual compounds. Using stably transformed *N. attenuata* plants silenced in jasmonate production and perception, or production of *N. attenuata* Hyp-rich glycopeptide systemin precursor by RNA interference, we identified malonylation as the key biosynthetic step regulated by herbivory and jasmonate signaling. We stably silenced *N. attenuata* geranylgeranyl diphosphate synthase (*ggpps*) to reduce precursors for the HGL-DTG skeleton, resulting in reduced total HGL-DTGs and greater vulnerability to native herbivores in the field. Larvae of the specialist tobacco hornworm (*Manduca sexta*) grew up to 10 times as large on *ggpps* silenced plants, and silenced plants suffered significantly more damage from herbivores in *N. attenuata*'s native habitat than did wild-type plants. We propose that high concentrations of HGL-DTGs effectively defend valuable tissues against herbivores and that malonylation may play an important role in regulating the distribution and storage of HGL-DTGs in plants.

INTRODUCTION

Diterpene glycosides (DTGs) are a diverse group of terpenoid metabolites known for their elaborate structures and potential medical and dietary applications in humans (for example, see Schiffman and Gatlin, 1993; Kim and Kinghorn, 2002; Gregersen et al., 2004; DeMarino et al., 2006). DTGs consist of a cyclic or acyclic diterpene (C_{20}) skeleton and attached sugar moieties that may bear additional functional groups. Stevioside, a cyclic DTG produced by stevia (*Stevia rebaudiana* Bertoni) and used as a sugar substitute, is 300 times as sweet as sugar (Hanson and De Oliveira, 1993) and inhibits monosaccharide metabolism in the rat liver (Ishii et al., 1987); capsianoside, a linear DTG with a hydroxygeranyllinalool skeleton from pepper (*Capsicum annuum*), may alter the permeability of intestinal tight junctions in human cell lines (Hashimoto et al., 1997). The term "terpenoid" encompasses all molecules derived from the condensation of the C5 precursor isopentenyl pyrophosphate (C_5) and its allylic isomer dimethylallyl pyrophosphate (C_5), which in higher plants are synthesized from one of two independent pathways: the mevalonic acid pathway in the cytosol or the 2-C-methyl-D-erythritol 4-phosphate/1-deoxy-D-xylulose 5-phosphate pathway in plastids (Lichtenthaler, 1999; Newman and Chappell, 1999; Towler and Weathers, 2007). Plastidial geranylgeranyl pyrophosphate synthases (GGPPSs) catalyze the condensation of three molecules of isopentenyl pyrophosphate with dimethylallyl pyrophosphate to produce the diterpenoid precursor geranylgeranyl pyrophosphate (GGPP; C_{20}) (Ohnuma et al., 1998; Dewick, 2002).

Hydroxygeranyllinalool (HGL)-DTGs consist of an acyclic C_{20} 17-hydroxygeranyllinalool skeleton conjugated to sugar groups (glucose and rhamnose) via bonds at C-3 and C-17 hydroxylated carbons; additional sugars are conjugated to the C'-2, C'-4, or C'-6 hydroxyl groups. Malonyl groups are typically connected to the C'-6hydroxyl group of the glucose(s) (Taguchi et al., 2005; Yu et al., 2008). HGL-DTGs have been isolated from many members of the *Solanaceae*, including tobacco (*Nicotiana* spp) (Shinozaki et al., 1996; Snook et al., 1997; Jassbi et al., 2006), *C. annuum* (Izumitani et al., 1990; Hashimoto et al., 1997; Lee et al., 2006, 2007, 2008; De Marino et al., 2006), and wolfberry (*Lycium*

[1] These authors contributed equally to this work.
[2] Current address: Chemistry Department, College of Letters and Sciences, University of Wisconsin, Madison, WI 53706.
[3] Current address: Department of Plant Nutrition, Leibniz Institute of Vegetable and Ornamental Crops, Grossbeeren, Germany 14979.
[4] Current address: Medicinal and Natural Products Chemistry Centre, University of Medical Sciences, Shiraz, Iran 71345.
[5] Address correspondence to baldwin@ice.mpg.de.
The author responsible for distribution of materials integral to the findings presented in this article in accordance with the policy described in the Instructions for Authors (www.plantcell.org) is: Ian T. Baldwin (baldwin@ice.mpg.de).
[W] Online version contains Web-only data.
www.plantcell.org/cgi/doi/10.1105/tpc.109.071449

chinense) (Terauchi et al., 1995, 1998). Snook et al. (1997) found HGL-DTGs to be highly abundant (>2.5% dry mass) in at least 26 *Nicotiana* species. Several studies have found negative correlations between total HGL-DTG content and the mass gained by lepidopteran larvae feeding on different species of *Nicotiana* (Lou and Baldwin, 2003), different cultivars of tobacco (*Nicotiana tabacum*) (Snook et al., 1997), or different transformed lines of the wild tobacco *Nicotiana attenuata* (Mitra et al., 2008). Larvae of the solanaceous specialist tobacco hornworm *Manduca sexta* reared on agar diets coated with isolated plant HGL-DTG fractions grew less than larvae reared on water-coated diets (Jassbi et al., 2006). Snook et al. (1997) showed that HGL-DTGs in artificial diet reduced the mass of *Heliothis virescens* larvae and that this required the intact double-bond structure of the HGL skeleton.

Little is known about the dynamics and regulation of HGL-DTGs in *N. attenuata* and other plants. HGL-DTGs are not found on the surface or in the trichomes of *N. attenuata* leaves (Roda et al., 2003), although other diterpenoids have been found in trichomes of *N. tabacum* (Lin and Wagner, 1994; Guo and Wagner, 1995). Concentrations of particular HGL-DTGs vary seasonally in flowers of *L. chinense* (Terauchi et al., 1997b). HGL-DTG biosynthesis depends on the production of GGPP in the plastid and sufficient free sugars and malonic acid and is thus likely correlated with photosynthesis. In *N. attenuata*, total HGL-DTG concentrations in leaves increase after treatment with the plant stress hormone methyl jasmonic acid (MJ) or feeding by *M. sexta* larvae (Keinänen et al., 2001; Jassbi et al., 2008).

A GGPPS characterized in *N. attenuata* (NaGGPPS) provides GGPP for HGL-DTG biosynthesis and plays a minimal role in primary metabolism (Jassbi et al., 2008). Jassbi et al. (2008) used transient virus-induced gene silencing (VIGS) of *ggpps* to reduce total HGL-DTG levels in *N. attenuata* plants and found that *M. sexta* larvae grew three times as large on VIGS-*ggpps* plants as on VIGS empty vector controls and significantly larger than larvae on VIGS-*pmt* (reduced nicotine) or VIGS-*tpi* plants (reduced trypsin protease inhibitors [TPIs]). Both nicotine and TPIs have a significant negative effect on *M. sexta* larval growth (Steppuhn et al., 2004; Zavala et al., 2004). HGL-DTGs are thus a potent defense against lepidopteran herbivores, but their regulation and mechanism of action in planta as well as their role in defense against plants' native herbivores have not been examined.

Most known herbivore-elicited defense metabolites are regulated by the jasmonate (JA) signaling pathway, which also mediates plant responses to abiotic stresses, such as UV radiation and ozone, and developmental processes, including tuberization, senescence, and reproductive development (Mueller et al., 1993; Creelman and Mullet, 1997; Lorenzo and Solano, 2005; Schilmiller and Howe, 2005; Wasternack, 2007). The first committed step in JA biosynthesis is the oxygenation of α-linolenic acid by a 13-lipoxygenase (LOX3 in *N. attenuata*) to the intermediate 13-HPOT (Vick and Zimmerman, 1984). Inverted repeat RNA interference (RNAi) lines deficient in *lox3* (IR*lox3*) have severely reduced levels of all JA hormones and are useful in revealing the role of JAs in coordinating induced defense responses (shown for antisense AS*lox3* lines in Halitschke and Baldwin, 2003). Some or all JAs effect signaling via interaction with the F-box protein COI1, a subunit of the SCF^{COI1} E3 ubiquitin ligase complex, which triggers the degradation of JAZ repressors of JA signaling and permits the transcription of JA-elicited genes (Xie et al., 1998; Chini et al., 2007; Thines et al., 2007; Chung et al., 2008; Ribot et al., 2008). Inverted repeat RNAi lines deficient in Na *coi1* (IR*coi1*) are impaired in both JA biosynthesis and perception because JAs stimulate their own biosynthesis (Paschold et al., 2007, 2008). Responses dependent on COI1-mediated JA perception can be identified by supplementing IR*lox3* and IR*coi1* plants with JAs and determining which responses are restored in IR*lox3*, but not in IR*coi1*. In general, plants deficient in LOX3 or COI1 are highly susceptible to attack from herbivores and pathogens (Reymond et al., 2000; Ellis and Turner 2002; Kessler et al., 2004; Li et al., 2004; Mewis et al., 2005; Chung et al., 2008).

The Hyp-rich systemin glycopeptides, encoded by a 146–amino acid precursor in tomato (*Solanum lycopersicum*) (Pearce et al., 2001), are wound-induced signals that trigger the induction of JA-mediated defenses. Two Hyp-rich systemin glycopeptides derived from a 165–amino acid systemin-like glycopeptide precursor have been reported in *N. tabacum* (Pearce et al., 2001; Ryan and Pearce, 2003), and a homolog of the *N. tabacum* precursor is known in *N. attenuata* (ppHS; Berger and Baldwin, 2007). Unlike the systemin-like glycopeptides in tomato (Pearce et al., 2009) and *N. tabacum* (Ren and Lu, 2006), Na ppHS does not play a central role in the induction of JA-mediated defense in vegetative tissues: inverted repeat Na ppHS lines (IR*sys*) are not more susceptible to native herbivores than are wild-type plants and have normal herbivore-elicited oxylipin dynamics (Berger and Baldwin, 2007). However, ppHS may influence JA signaling in flowers (Berger and Baldwin, 2009). Recently, Pearce et al. (2009) isolated a homolog of the tobacco and tomato Hyp-rich systemin glycopeptides from black nightshade (*Solanum nigrum*) and showed that this peptide may be involved in early JA signaling.

We identified several HGL-DTGs previously unknown in *N. attenuata*, bringing the total number to 11 in this species. We characterized the accumulation of these compounds in vegetative and reproductive plant tissues and followed their dynamics in plants that were left unelicited or elicited with wounding and *M. sexta* oral secretions (W+OS). Using IR*sys*, IR*lox3*, and IR*coi1* plants, we determined the roles of ppHS and JA signaling in the herbivore-induced dynamics of individual HGL-DTGs. Lines stably silenced in *ggpps* (IR*ggpps*) allowed us to assess the effect of total HGL-DTGs on the specialist *M. sexta* and generalist herbivores in *N. attenuata*'s native habitat. Given that IR*sys* plants, which we show to be impaired in the JA-mediated accumulation of malonylated HGL-DTGs, are not more susceptible to native herbivores (Berger and Baldwin, 2007), we discuss the importance of total HGL-DTGs as a defense and the possible roles of malonylation in the metabolism of HGL-DTGs.

RESULTS

Identification, Analysis, and Structure of HGL-DTGs in *N. attenuata*

We identified eleven HGL-DTGs that are highly abundant in aboveground tissues of *N. attenuata* (Figure 1; see Supplemental

A

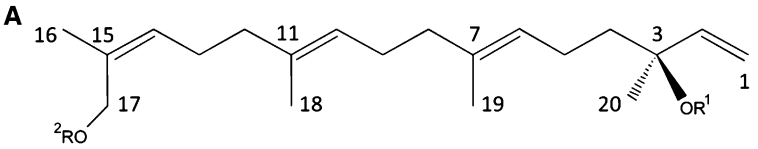

		R1		R2		Malonyl-
	Group*	Sugar 1	Sugar 2	Sugar 1	Sugar 2	groups
Lyciumoside I	1	Glc		Glc		
Lyciumoside II	1	Glc		Glc	Glc	
Lyciumoside IV	2	Glc	Rh	Glc		
Nicotianoside I	3	Glc	Rh	Glc		**1**
Nicotianoside II	4	Glc	Rh	Glc		**2**
Nicotianoside III	2	Glc	Rh	Glc	Rh	
Nicotianoside IV	3	Glc	Rh	Glc	Rh	**1**
Nicotianoside V	4	Glc	Rh	Glc	Rh	**2**
Attenoside	2	Glc	Rh	Glc	Glc	
Nicotianoside VI	3	Glc	Rh	Glc	Glc	**1**
Nicotianoside VII	4	Glc	Rh	Glc	Glc	**2**

* 1 Precursor 2 Core 3 Malonylated 4 Dimalonylated

B

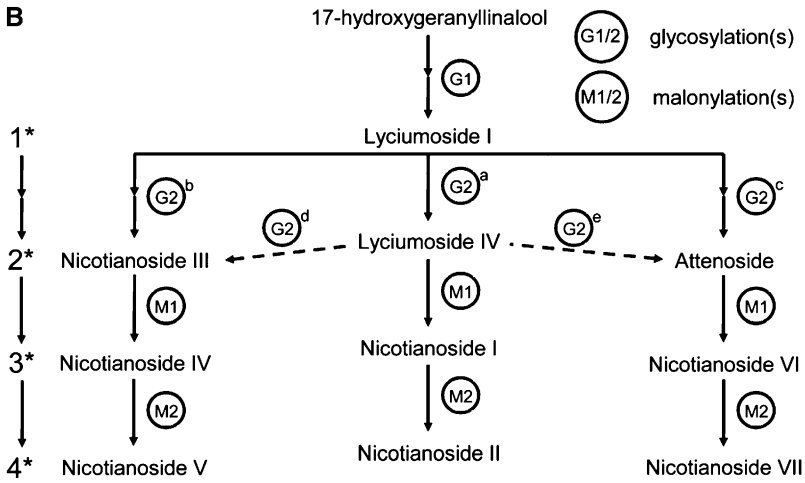

Figure 1. Identity and Biosynthesis of HGL-DTGs.

(A) Newly identified and previously described compounds from leaves of *N. attenuata* differing in their sugar and malonyl groups are organized into the following biosynthetic groups: (1) precursor, (2) core, (3) singly malonylated, and (4) dimalonylated compounds. Rh, rhamnose; Glc, glucose.

(B) Biosynthetic pathway: HGL is glycosylated at the C-3 and C-17 hydroxyl groups to lyciumoside I, the precursor for all HGL-DTGs. Additional glycosylations of lyciumoside I (G2a, b, and c) or lyciumoside IV (G2d and e) produce larger core HGL-DTGs that may be malonylated once (M1) or twice (M2). 1*, 2*, 3*, and 4* refer to the group in **(A)**.

Tables 1 and 2 online). HGL-DTGs differ in their sugar moieties and number of malonyl sugar esters (0-2) and can be divided into three classes: the precursor lyciumoside I, core molecules that are fully glycosylated but have no malonyl groups (lyciumoside IV, nicotianoside III, and attenoside), singly malonylated compounds (nicotianosides I, IV, and VI), and dimalonylated compounds (nicotianosides II, V, and VII) (Figure 1). Malonylated HGL-DTGs are poorly described (Terauchi et al., 1998). We optimized the buffer composition (see Supplemental Figure 1 online) and dilution of our extraction to maximize the yield of each individual compound; 40% methanol at a slightly acidic pH was the best compromise that maximized the yield of more water-soluble (precursor and core) and less water-soluble (malonylated) compounds and their ionization in liquid chromatography–mass spectrometry measurements. Samples were diluted 50 times to ensure that all compounds were measured in the linear range. From standard addition curves, we calculated that the most abundant HGL-DTGs are present at a concentration of 1 to 5 mg/g fresh mass (FM) in wild-type leaf tissue (see Supplemental Figure 2 online). We tested the durability and robustness of signal mass detection and the reproducibility of extraction and measurement conditions by analyzing injection replicates of an single leaf extract (n = 20). Reproducibility of extraction and measurement conditions was confirmed (relative standard deviation lower than 10%) for all but one HGL-DTG and for two internal standards (glycyrrhizinic acid and ^{2}D jasmonic

acid): attenoside had a higher error (relative standard deviation 21%).

Ontogeny of HGL-DTG Accumulation

We analyzed the distribution of HGL-DTG accumulation in aboveground tissues of *N. attenuata* plants at different growth stages (rosette, elongated, younger, and older flowering plants) that had been left unelicited (control) or elicited with W+OS (wounding plus *M. sexta* larval oral secretions [OS]) to mimic herbivory with a precisely defined kinetic. In a previous experiment, no HGL-DTGs were found in roots of rosette-stage plants treated with W+OS 3 d after treatment (data not shown).

Plants' total pools of HGL-DTGs increased during growth until plants began to flower (Figure 2A): elongated plants produced more total HGL-DTGs than did rosette plants (multiple *t* tests with Bonferroni-corrected P's; $P \leq 0.001$), and young flowering plants produced more than elongated plants ($P \leq 0.001$) regardless of treatment. Old flowering plants had 6 to 8 times the total HGL-DTG content as rosette-stage plants but did not contain more total HGL-DTGs than young flowering plants ($P > 0.075$). Because young flowering plants contained the most vegetative and reproductive tissue types (only the ripe seed capsules were missing from this stage of growth) and still responded dynamically to W+OS elicitation, we present the allometrically corrected distribution of HGL-DTGs in this growth stage (Figure 2B; allometric correction explained in Baldwin, 1996).

The distribution of HGL-DTGs varied greatly among tissue types, ranging from nearly undetectable levels in stems to the highest concentrations in young leaves and reproductive organs. The ratio of mono- to dimalonylated DTGs was markedly different in reproductive tissues versus leaves. While dimalonylated HGL-DTGs were more abundant in leaves, singly malonylated compounds dominated the pools of buds, calyxes, and flowers. For young flowering plants, the percentage of total HGL-DTGs in each tissue type was calculated and compared with the percentage of mass that different tissues represent in the plant to derive the normalized tissue-specific pools. This presentation reveals that HGL-DTGs are preferentially allocated to young and reproductive tissues (Table 1).

A single W+OS elicitation changed the allocation of HGL-DTGs in individual tissues but did not significantly change the whole-plant pool for any growth stage. Concentrations of singly malonylated HGL-DTGs increased in the elicited leaf of elongated and young flowering plants (individual *t* tests; elongated, $P = 0.010$; young flowering, $P = 0.031$), whereas levels of core compounds increased in calyxes of W+OS-elicited young flowering plants ($P = 0.044$). There was no significant increase in the other HGL-DTG classes in elicited leaves and no significant changes in any HGL-DTGs in elicited leaves of rosette-stage or old flowering plants.

Accumulation of *ggpps* transcripts in young flowering plants was found to be highest in buds, followed by green leaves (rosette and stem leaves had similar levels; Figure 3). Senescing leaves accumulated fewer *ggpps* transcripts, likely due to their loss of active chloroplasts, and roots and stems had only very low levels (analysis of variance [ANOVA], $F_{6,20} = 28.30$, $P < 0.0001$). Thus, the expression of *ggpps* correlates well with the relative concentrations of HGL-DTGs in different tissues.

Kinetics of HGL-DTG Biosynthesis and Elicitation

We analyzed the kinetics of HGL-DTG accumulation over 1 week in five green leaves of rosette-stage control and W+OS-elicited plants. Each biosynthetic group showed a distinct pattern of constitutive and W+OS-elicited dynamics that can be described as follows: concentrations of the precursor lyciumoside I always increased first and then fell as concentrations of core compounds increased; core compounds then stabilized as concentrations of malonylated compounds increased; and W+OS elicitation significantly increased the rate of biosynthesis of core and malonylated compounds (Student's *t* tests; Figure 4; see Supplemental Table 3 online). By the end of the experiment, concentrations of all core and malonylated HGL-DTGs except attenoside and nicotianoside II had increased significantly, whereas the precursor lyciumoside I had returned to initial levels (unpaired *t* tests between the first and the last time point in control plants: nicotianoside II, $P = 0.108$; attenoside, $P = 0.067$; lyciumoside I, $P = 0.137$; all others, $P < 0.05$).

In W+OS-elicited leaves, accelerated biosynthesis of HGL-DTGs apparently resulted in a greater accumulation of the precursor lyciumoside I, leading to sustained increases in malonylated compounds above control levels. Malonylated and dimalonylated HGL-DTGs first accumulated in W+OS-elicited leaves by 14 h: >6 d earlier than in control leaves. Concentrations of lyciumoside I were lower in W+OS-elicited than in control leaves at 1 h but increased to concentrations much greater than in control leaves by 14 h before returning to control levels. Interestingly, lyciumoside I concentrations also peaked at 14 h in control leaves: as this was the only night time harvest, it suggests that precursors increase in concentrations during the night.

The core compounds lyciumoside IV and nicotianoside III accumulated similarly in elicited and control leaves until 3 d (although levels of lyciumoside IV were somewhat higher in control leaves 1 h after treatment) but then stabilized, whereas concentrations in control leaves continued to increase until day 5 and then fell concurrent with the rise in control levels of malonylated compounds at day 7. Among the core compounds, attenoside was the exception: concentrations were lower in elicited leaves beginning at 14 h. The missing attenoside could have been routed to synthesis of nicotianoside VII, its dimalonylated adduct, which was not determined in this experiment. The singly malonylated adduct of attenoside, nicotianoside VI, was the only malonylated compound that accumulated no differently in W+OS-elicited leaves.

JA and ppHS Signaling Are Required for HGL-DTG Biosynthesis

Wild-type plants and lines silenced in JA (IR*lox3* and IR*coi1*) and ppHS signaling (IR*sys*) were elicitated with W+OS or JA supplementation with MJ in lanolin paste (lan+MJ). Concentrations of malonylated HGL-DTGs increased after W+OS or lan+MJ treatment in wild-type leaves compared with control or lanolin (lan)-treated plants; precursor and core compounds decreased or

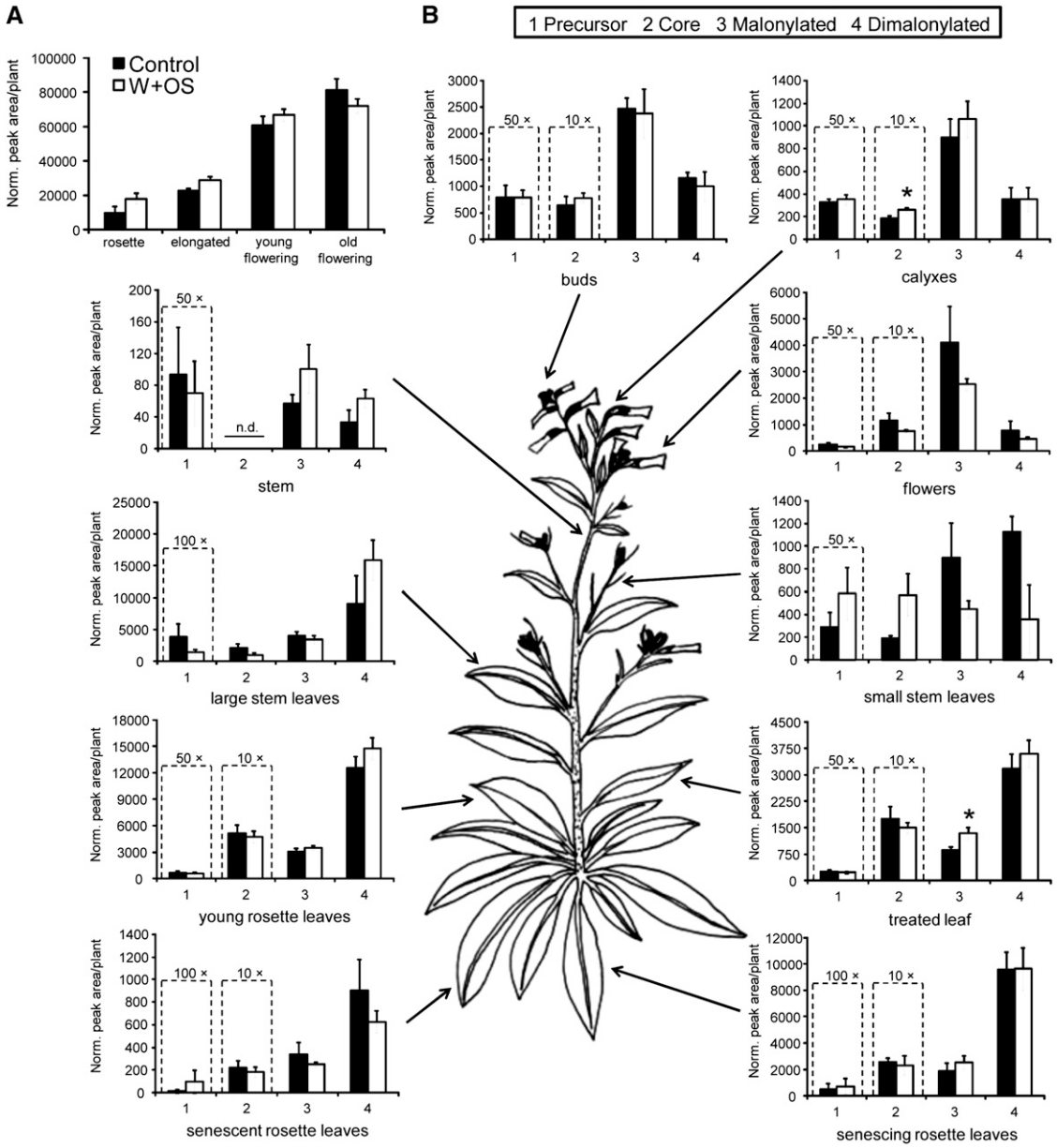

Figure 2. *N. attenuata* Accumulates HGL-DTGs during Growth and Differentially Accumulates Them to Young and Reproductive Tissues.

Plants were left unelicited (Control), or one leaf per plant was elicited with wounding and *M. sexta* oral secretions (W+OS). Aboveground tissues were harvested 3 d after treatment and pooled by tissue type. In a previous experiment, no HGL-DTGs were found in roots (data not shown). Note that some compounds have been multiplied by constants to fit the scale of the graph and that scales change among graphs. *P < 0.05 in a Student's *t* test. n.d., not detected.

(A) HGL-DTGs (average + SE) accumulate as plants grow from the rosette stage (34 d old) and elongate (44 d old) through the initiation of flowering; total HGL-DTG pools are no different in young (54 d old) versus old (68 d) flowering plants (n = 4 plants).

(B) Accumulation of HGL-DTGs in a young flowering plant. Singly malonylated compounds accumulate in reproductive tissues, whereas doubly malonylated compounds accumulate in leaves. The greatest amounts of HGL-DTGs are found in young and reproductive tissues. W+OS elicitation of a leaf changes the composition of HGL-DTGs in that leaf, likely by reallocation from the rest of the plant because a single treatment has no significant effect on total HGL-DTG pools in **(A)**.

Table 1. Normalized Tissue-Specific Pools of HGL-DTGs in Aboveground Tissues of Young Flowering (54 d old) Plants

Tissue	Normalized Tissue-Specific Pool (% Total HGL-DTGs/% Total FM)
Senescent rosette leaves	31
Senescing rosette leaves	99
Young rosette leaves	170
Elicited leaf position (S1)[a]	223
Large stem leaves	265
Small stem leaves	277
Calyxes	215
Flowers	296
Buds	430

[a]First stem leaf. Tissue types are defined in Figure 2B.

remained constant (see Supplemental Figure 3 online; ANOVA and Bonferroni post-hoc test results are in Supplemental Tables 4 and 5 online). The malonylated adducts of attenoside behaved differently than the other malonylated DTGs in that they increased more after W+OS than after lan+MJ treatment, suggesting that the metabolism of attenoside is not entirely JA dependent or that nicotianosides VI and VII become substrates for unknown JA-inducible product(s). For all genotypes, all differences that were significant between lan and lan+MJ-treated plants were also significant between control and lan+MJ-treated plants except for nicotianoside IV and nicotianoside VI in the wild type, and lan treatment did not affect control levels of HGL-DTGs (see Supplemental Table 6 online).

JA and ppHS-silenced lines did not display wild-type accumulation of HGL-DTGs in leaves at 3 d after elicitation (Figure 5), when most induced changes in HGL-DTG metabolism are stable (Figure 4). The signaling mutants IR*lox3*, IR*coi1*, and IR*sys* all had reduced levels of malonylated HGL-DTGs, but this phenotype was far stronger in the JA-silenced lines IR*lox3* and IR*coi1* (Figure 5; see Supplemental Figure 3 online; ANOVA and Bonferroni post-hoc test results are in Supplemental Tables 4 to 7 online). In IR*lox3*, reduced levels of malonylated compounds after W+OS elicitation could be fully recovered by lan+MJ treatment for singly malonylated and partially recovered for dimalonylated HGL-DTGs. Lan+MJ treatment could not recover singly or dimalonylated HGL-DTGs in IR*coi1* plants, which had the greatest reduction in malonylated compounds and nearly undetectable levels of dimalonylated compounds. Thus, malonylation is strongly dependent on JA biosynthesis and perception, and higher levels of perceived JAs are required to add the second malonyl moiety; ppHS also influences the second malonylation step.

Whereas both COI1 and LOX3 are required for malonylation, COI1, but not LOX3, is involved in glycosylation of lyciumoside I to generate core compounds. Core compounds decreased in wild-type leaves after treatment with W+OS and lan+MJ (except for attenoside after W+OS and nicotianoside III after lan+MJ) but accumulated in IR*lox3* plants without lan+MJ treatment (see Supplemental Tables 4 and 5 online; Figure 5). IR*coi1* had reduced levels of core compounds other than attenoside in control leaves, but near-wild-type levels after W+OS elicitation. Lan+MJ treatment recovered concentrations of core molecules to wild-type levels in IR*coi1* leaves, likely due to an increase in the precursor pool rather than an increase in precursor glycosylation. Interestingly, concentrations of attenoside were not reduced in IR*coi1* leaves and were greater than wild-type concentrations after W+OS and lan+MJ. IR*lox3* plants had wild-type levels of lyciumoside I, but IR*coi1* plants had concentrations 3.75 times greater than the wild type after W+OS and 4.5 times greater after lan+MJ. In wild-type leaves, the precursor lyciumoside I decreased after treatment with W+OS but did not change after treatment with lan+MJ (see Supplemental Table 5 online; Figures 5A and 5D). Control leaves of IR*sys* plants also had higher concentrations of lyciumoside I (see Supplemental Table 7 online; Figure 5D).

Only the combination of deficient JA biosynthesis and perception in IR*coi1* strongly influenced total levels of HGL-DTGs (Figure 6): both IR*lox3* plants and IR*coi1* plants had lower levels of HGL-DTGs, but the difference between IR*lox3* and the wild type was no longer significant following W+OS elicitation (Figure 6A) due to accumulation of core molecules by IR*lox3* (Figures 5A to 5C). Accumulation of precursors in IR*coi1* plants did not compensate for their reduced production of most core and all malonylated compounds (Figures 5A to 5C and 6A; $P < 0.001$). After lan+MJ treatment, total HGL-DTG levels were identical in the wild type and IR*lox3*, but still strongly reduced in IR*coi1* plants ($P < 0.001$). IR*sys* plants were not impaired in total HGL-DTG accumulation (Figure 6B).

Stably Silencing *ggpps* Reduces Total HGL-DTGs in *N. attenuata* with Minimal Nontarget Effects

Although silencing *ggpps* may have unwanted effects on other GGPP-dependent metabolites, such as carotenoids, we concluded that it is the best gene target for knocking down total HGL-DTG production in *N. attenuata*. Other potential targets for reducing levels of total HGL-DTGs include enzymes that convert GGPPS to the HGL-DTG skeleton: geranyllinalool synthase and a cytochrome p450, which hydroxylates geranyllinalool. Silencing geranyllinalool synthase could produce a buildup of GGPP, which might result in the formation of other diterpene toxins or antifeedants, and worse, silencing the Cyp450 would likely

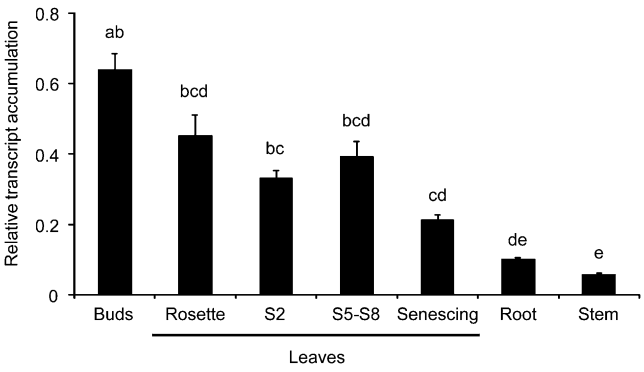

Figure 3. *ggpps* Transcript Accumulation in Tissues of Young Flowering Plants (54 d old) Relative to *N. attenuata actin* (average + SE; $n = 4$ Plants).

Different letters indicate significant differences ($P < 0.05$) in Bonferroni-corrected post-hoc tests following an ANOVA.

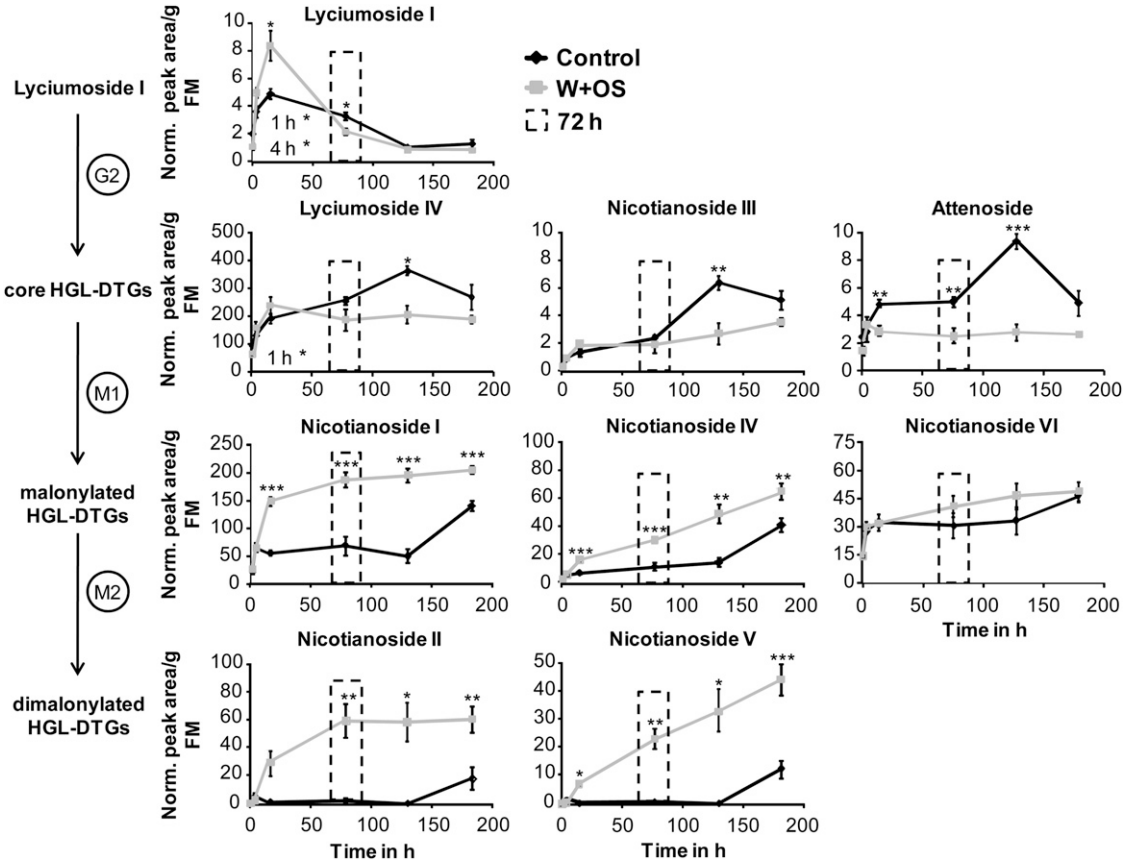

Figure 4. The Different Biosynthetic Groups of HGL-DTGs Display Characteristic Dynamic Patterns over 1 Week of Growth in Rosette-Stage Plants.

Plants were left unelicited (Control), or five leaves per plant were elicited with W+OS. Elicited leaf positions were harvested and pooled from each plant (one pooled sample per plant, $n = 5$) at one of five time points: 1, 4, and 14 h (night), and 3, 5, and 7 d. The precursor lyciumoside I (average + SE) attains maximum concentration during the night at 14 h and then decreases as other compounds accumulate. In W+OS-elicited leaves, the sharp decline in precursor levels following their 14 h peak likely supply substrates for the subsequent accumulation of core compounds, which do not peak, but are maintained at a constant level as they provide substrate for the synthesis of malonylated compounds. The elevation in malonylated compounds begins concurrently with the elevation in core compounds and precursor levels in W+OS-elicited leaves, but at 7 d in unelicited leaves. All compounds reach stable elicited levels beginning at 3 d after W+OS elicitation (indicated by the dotted rectangle) with the exception of malonylated compounds derived from nicotianoside III, which continue to increase. Note that scales change among graphs. Asterisks indicate significant differences between W+OS-treated and control samples in Student's *t* tests within each time point (*$P \leq 0.05$, ** $P < 0.01$, and *** $P < 0.001$).

produce elevated levels of geranyllinalool, which can be toxic to insects (Lemaire et al., 1990).

In our experiments, we were careful to monitor plant growth and levels of nontarget defensive metabolites during all bioassays. As demonstrated in pictures and by growth and defensive metabolite data from glasshouse and field-grown plants (Figures 7 and 8; see Supplemental Figures 5 to 7 online), the main difference between IR*ggpps* and wild-type plants during the time over which we conducted bioassays was the level of HGL-DTGs. Data from a competition assay in the glasshouse (see Supplemental Figure 4 online) confirm that IR*ggpps* plants grow normally and do not suffer a reduction in seed production under glasshouse conditions, implying that there is no strong effect of silencing *ggpps* on primary metabolism. To the extent that IR*ggpps* plants accumulate less of any primary metabolites, the comparison of herbivore damage and growth on IR*ggpps* versus wild-type plants provides a conservative estimation of the defensive effect of HGL-DTGs. Thus, in the worst case, silencing *ggpps* underestimates rather than inflates our estimation of the importance of HGL-DTGs in plant defense.

HGL-DTGs Dramatically Increase Resistance against a Specialist Herbivore

M. sexta larvae were fed on wild-type plants or one of two independently silenced lines of IR*ggpps* for 13 d (silencing efficiency line 1, 69.7% ± 4.5%; line 2, 94.2% ± 1.0%; see Supplemental Figure 5A online). Mortality of *M. sexta* larva on IR*ggpps* lines was one-quarter to one-half of that on wild-type plants (26% on IR*ggpps* line 1, 13% on IR*ggpps* line 2, and 52% on the wild type). Larvae on either IR*ggpps* line gained up to 10 times as much mass as those that survived on the wild type; there

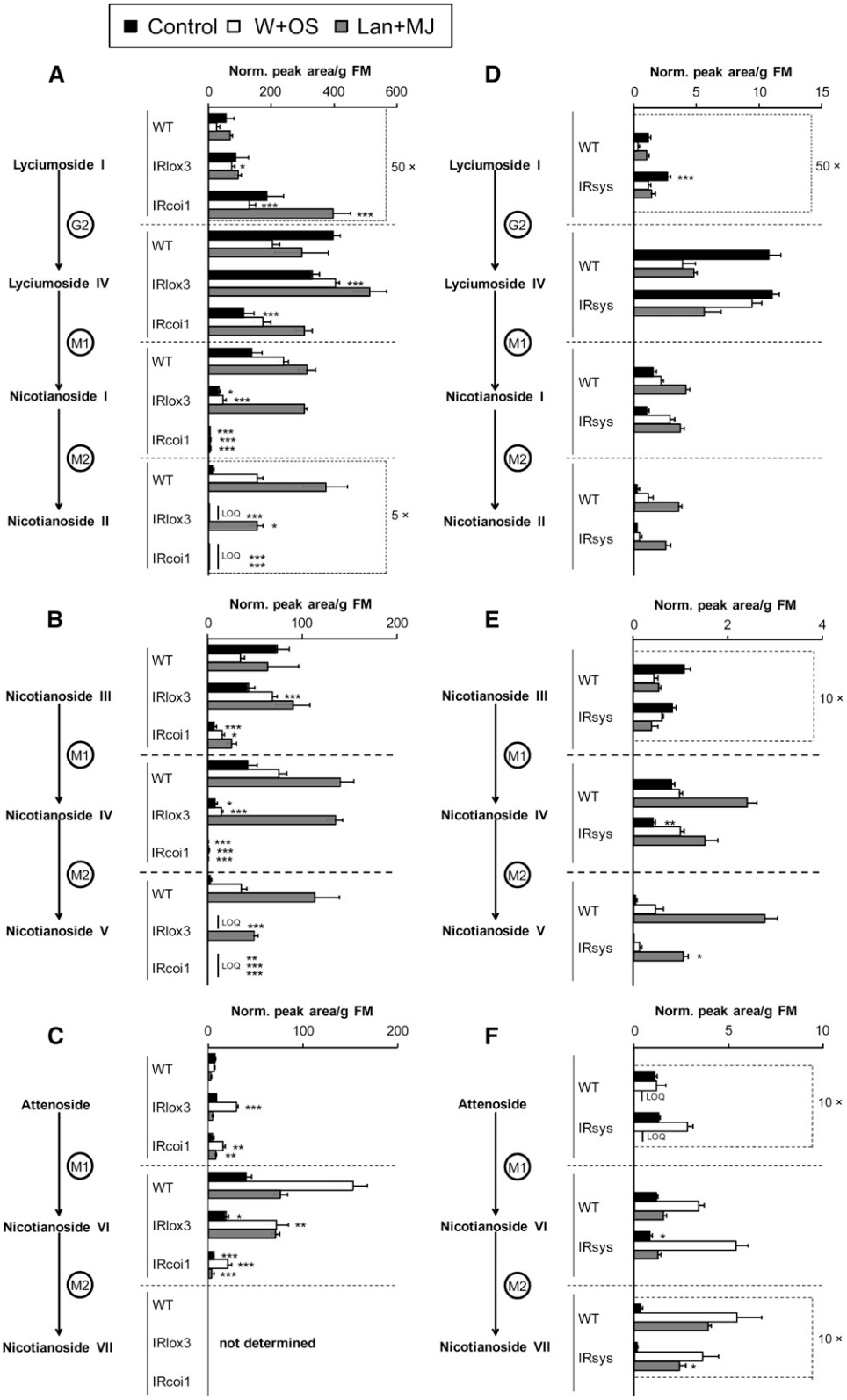

Figure 5. Malonylation of HGL-DTGs Is Regulated by JA Signaling and Tuned by ppHS Signaling.

(A) to **(C)** Experiment 1: wild type, IR*lox3*, and IR*coi1*.

was no difference in the average mass of larvae feeding on IR*ggpps* line 1 or 2 (Figure 7A; repeated-measures ANOVA followed by Bonferroni post-hoc tests, $F_{6,32} = 10.76$, $P < 0.0001$).

HGL-DTGs are likely responsible for the dramatic difference in larval mass on IR*ggpps* versus wild-type plants as all other secondary metabolites known to influence *M. sexta* growth were not altered in IR*ggpps* plants. Levels of all types of HGL-DTGs in lan (control) or lan+MJ-treated leaves were consistently lower for both lines of IR*ggpps* than for the wild type, although the difference in levels of dimalonylated compounds, which were present in low concentrations and were highly variable in wild-type leaves, was not always statistically significant (Figures 7B to 7D; ANOVAs within treatment followed by Bonferroni post-hoc tests; total HGL-DTGs, lan, $F_{2,11} = 17.9$, $P < 0.001$; lan+MJ, $F_{2,11} = 51.4$, $P < 0.001$; for individual compounds, see Supplemental Table 8 online and Figures 7C to 7E). Other defense-related metabolites were similar to wild-type levels in IR*ggpps* plants, although nicotine was slightly higher and chlorogenic acid slightly lower, and IR*ggpps* plants grew similarly to wild-type plants in both the field as well as in the glasshouse (see Supplemental Figures 4, 5B to 5E, 6, and 7 online; results of paired *t* tests for growth and fitness are in Supplemental Table 9 online; ANOVAs within each treatment for secondary metabolites: TPI, lan, $F_{2,10} = 3.50$, $P = 0.066$; lan+MJ, $F_{2,10} = 3.45$, $P = 0.073$; nicotine, lan, $F_{2,11} = 5.90$, $P = 0.018$; lan+MJ, $F_{2,10} = 12.5$, $P = 0.002$; rutin, lan, $F_{2,11} = 19.1$, $P < 0.001$; lan+MJ, $F_{2,10} = 8.67$, $P = 0.007$; chlorogenic acid, lan, $F_{2,11} = 2.57$, $P = 0.121$; lan+MJ, $F_{2,10} = 4.20$, $P = 0.047$).

Plants Deficient in HGL-DTGs Are More Susceptible to Herbivores in Nature

IR*ggpps* Line 1 plants were grown in a paired design with wild-type plants in a field plot experiment in *N. attenuata*'s native habitat, and damage by native herbivores was observed for 11 d; at the end of this period, tissue samples were taken for analysis of secondary metabolites. Field-grown IR*ggpps* plants produced significantly lower concentrations of HGL-DTGs and received significantly greater damage from native herbivores, which could indicate decreased resistance or increased apparancy to herbivores. However, there was no observed difference in herbivore presence on IR*ggpps* versus wild-type plants, indicating that plants were equally apparent to herbivores and that increased damage on IR*ggpps* was due to its increased palatability. When herbivore attack was at its highest (May 16th), IR*ggpps* line 1 received significantly more damage from both abundant mirids (*Tupiocoris notatus*) and less abundant grasshoppers (*Trimeropteris* spp) than did wild-type plants (Figures 8A and 8B; mirids; paired *t* test, $P = 0.029$; grasshoppers; Wilcoxon sign-rank test, $P = 0.043$). IR*ggpps* also tended to receive more damage from flea beetles (*Epitrix* spp), which damaged IR*ggpps* plants before beginning to damage their wild-type neighbors. The difference in flea beetle damage between the wild type and IR*ggpps* was at a maximum but was not statistically significant on May 8th (Figure 8C).

Levels of all types of HGL-DTGs were consistently lower in IR*ggpps* line 1 than in the wild type, although the difference in levels of malonylated compounds, which were present in lower concentrations and were highly variable in wild-type leaves, was not always statistically significant (Figures 8D to 8G; paired *t* tests; total HGL-DTGs: $P = 0.003$; nicotianoside II, $P = 0.057$; nicotianosides IV and V, below the limit of quantification; nicotianoside VI, $P = 0.364$; all others, $P < 0.05$). There was no significant difference between IR*ggpps* line 1 and the wild type in any other defense-related metabolite on May 15th (see Supplemental Figure 6 online). Plants in a pair were of similar size, but IR*ggpps* plants grew slightly faster than the wild type and were taller by the end of the season, when herbivore damage was no longer monitored (see Supplemental Figure 7 online; paired *t* tests: stalk length May 22nd, $P = 0.003$; maximum rosette diameter May 6th, $P = 0.005$, May 7th, $P = 0.040$).

DISCUSSION

In this study, we have described the dynamic biosynthesis of HGL-DTGs abundant in the wild tobacco *N. attenuata* and

Figure 5. (continued).

(D) to **(F)** Experiment 2: IR*sys* and the wild type.

Elongated *N. attenuata* plants were left unelicited (Control), or one leaf per plant was elicited with W+OS to mimic herbivory, with 150 μg MJ in lanolin paste to supplement JA production. Elicited leaves were harvested at 3 d. Plants impaired in JA biosynthesis (IR*lox3*) and perception (IR*coi1*) or in systemin-mediated signaling (IR*sys*) were compared with wild-type plants in two separate experiments using identical methods. In this figure, we compare levels of each HGL-DTG among silenced lines and the wild type, which have received the same treatment. Lanolin paste (lan) was used to control for solvent effects for the lan+MJ treatment, and the effects of treatments within genotypes are shown in Supplemental Figure 3 and Supplemental Tables 4 and 5 online. Asterisks indicate significant differences from the wild type in one-way ANOVAs (wild type, IR*lox3*, and IR*coi1*; **[A]** to **[C]**) or Student's *t* tests (wild type and IR*sys*; **[D]** to **[F]**) within each treatment: *$P \leq 0.05$, ** $P < 0.01$, and *** $P < 0.001$ in Bonferroni-corrected tests. (Student's *t* tests were also subjected to the Bonferroni comparison as the same data were used to analyze the effect of treatment on HGL-DTG accumulation within genotypes.) Each graph represents the full biosynthetic pathway from glycosylation through malonylation for one set of HGL-DTGs. For example, in **(A)**, IR*coi1* plants accumulate the precursor lyciumoside I (average + SE; $n = 5$ plants) and are impaired in their ability to convert it to the core compound lyciumoside IV at a wild-type rate, especially after lan+MJ treatment; IR*lox3* plants accumulate lyciumoside IV, especially after W+OS elicitation. Both IR*coi1* and IR*lox3* are unable to malonylate lyciumoside IV in control and W+OS-elicited leaves. Malonylation is recovered in IR*lox3* and not in IR*coi1* by lan+MJ. By contrast, in **(D)**, IR*sys* plants are able to synthesize wild-type levels of lyciumosides IV and nicotianosides I and II, but like IR*coi1*, accumulate lyciumoside I in unelicited tissue; however, in **(E)** and **(F)**, IR*sys* plants are unable to accumulate wild-type levels of other dimalonylated HGL-DTGs (nicotianosides V and VII) after lan+MJ treatment. Note that some compounds have been multiplied by constants to fit the scale of the graph and that scales change among graphs. LOQ, below limit of quantification.

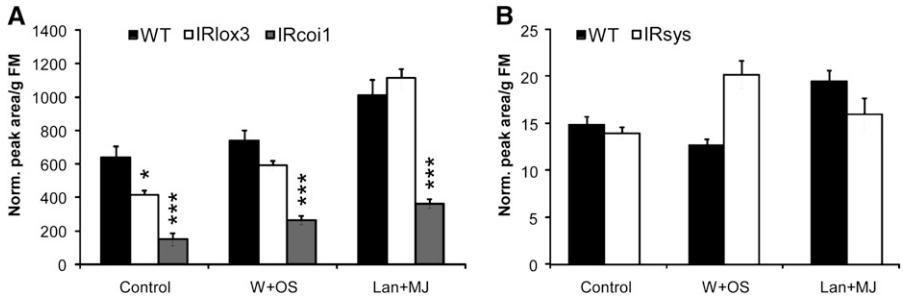

Figure 6. Total HGL-DTG Accumulation (Average + SE; $n = 5$ Plants) Requires JA Perception as Mediated by COI1.

Total HGL-DTGs were measured after no treatment (control) or treatment with W+OS or lan+MJ in wild-type, IR*lox3*, and IR*coi1* leaves in one experiment and in wild-type versus IR*sys* leaves in a replicate experiment conducted under the same conditions. Asterisks indicate significant differences from the wild type in a one-way ANOVA followed by Bonferroni-corrected tests (wild type, IR*lox3*, and IR*coi1*; **[A]**) or Student's *t* tests (the wild type and IR*sys*; **[B]**) within each treatment: *P ≤ 0.05, ** P < 0.01, and *** P < 0.001.

(A) Experiment 1: IR*lox3* accumulates nearly wild-type levels of HGL-DTGs after W+OS elicitation due to buildup of core compounds (Figure 5) and is completely restored to wild-type levels by lan+MJ treatment; neither W+OS nor lan+MJ treatment restores total HGL-DTG levels in IR*coi1*.

(B) Experiment 2: IR*sys* plants are not impaired in the accumulation of total HGL-DTGs.

highlighted glycosylation and malonylation as the key biosynthetic steps producing the diversity of compounds observed (Figure 1). Optimal defense theory (ODT) predicts that plant parts with the highest fitness value, such as reproductive organs, should be the best defended (McKey, 1979; Rhoades, 1979), and we suggest that the distribution of HGL-DTGs in *N. attenuata* corresponds to the predictions of ODT in that HGL-DTGs accumulate most in young and reproductive tissues (Figures 2B and 3). Field and glasshouse bioassays with IR*ggpps* plants showed that the reduction of total HGL-DTGs has a highly significant impact on the growth of, and damage inflicted by, multiple native herbivores of *N. attenuata* (Figures 7 and 8). Here, we discuss the roles of JA and ppHS signaling in the biosynthesis of HGL-DTGs, particularly in their malonylation, and the likely contributions of total versus malonylated compounds to defense (Figure 9). We propose that malonylation is primarily a mechanism for plants to regulate HGL-DTG accumulation and distribution, which according to ODT is vital to the defensive value of these compounds.

Dynamics of HGL-DTG Biosynthesis

Plants accumulate HGL-DTGs as they grow (Figure 2A); hence, their pool sizes need to be analyzed allometrically and concentrations can be compared only between plants at the same stage of growth with the same distribution of plant parts (for example, see Baldwin and Schmelz, 1996 for an allometric analysis of nicotine production). The accumulation of HGL-DTGs in whole plants differs for each biosynthetic class (Figures 1 and 2): malonylated compounds generally accumulate more than core or precursor molecules; singly malonylated compounds accumulate to higher levels in reproductive tissues, and dimalonylated compounds accumulate in leaves. The biosynthesis of malonylated compounds takes between 6 and 7 d in unelicited leaves, but begins only 14 h following W+OS elicitation. Three days after W+OS elicitation, the elicited leaves of rosette-stage (Figure 4), elongated (Figure 5, WT), and young flowering plants (Figure 2B) contain significantly higher levels of malonylated HGL-DTGs. This may result from transport from neighboring tissues or local biosynthesis: W+OS elicitation to multiple leaves significantly elevated precursor levels in those leaves (Figure 4).

Wild *Nicotiana* plants also accumulate nicotine in a similar pattern to HGL-DTGs: total pools increase as they grow, preferentially in young and reproductive tissues, and damage or JA application increases the rate of accumulation (Baldwin and Schmelz, 1996; Baldwin, 1999; Ohnmeiss and Baldwin, 2000). HGL-DTGs display a similar kinetic to nicotine, which reaches maximum levels 5 d following wounding or JA elicitation (Baldwin, 1999). Because nicotine is synthesized in roots, the eliciting JA signal must be transported from leaves to roots and the synthesized nicotine transported from roots back to leaves; HGL-DTGs may have a similar mechanism of elicitation but respond with a faster kinetic, where induced changes are stable within 3 d because they are synthesized in leaf tissues (Figure 3).

JAs Regulate HGL-DTG Biosynthesis in *N. attenuata*

Comparison of the accumulation of each HGL-DTG in wild-type plants and plants deficient either in JA biosynthesis (IR*lox3*) or both biosynthesis and perception (IR*coi1*) revealed separate but overlapping roles for *lox3* and *coi1* in the regulation of HGL-DTG biosynthesis (Figure 5). Neither JA mutant was able to induce wild-type levels of malonylated compounds in W+OS-elicited leaves, but this phenotype was more severe in IR*coi1* than in IR*lox3*. IR*lox3* plants accumulated core compounds, whereas IR*coi1* plants accumulated the precursor lyciumoside I (and attenoside; Figure 5C). JA supplementation with lan+MJ recovered most compounds to wild-type levels in IR*lox3*, but not in IR*coi1*. Dimalonylated compounds could not be fully recovered in IR*lox3*, indicating that their induced synthesis depends on a sustained or amplified JA signal resulting from the positive feedback of JAs on their own biosynthesis, which occurs in the wild type, but not in IR*lox3* plants. Because IR*coi1* plants were able to accumulate similar levels of core compounds as wild-type

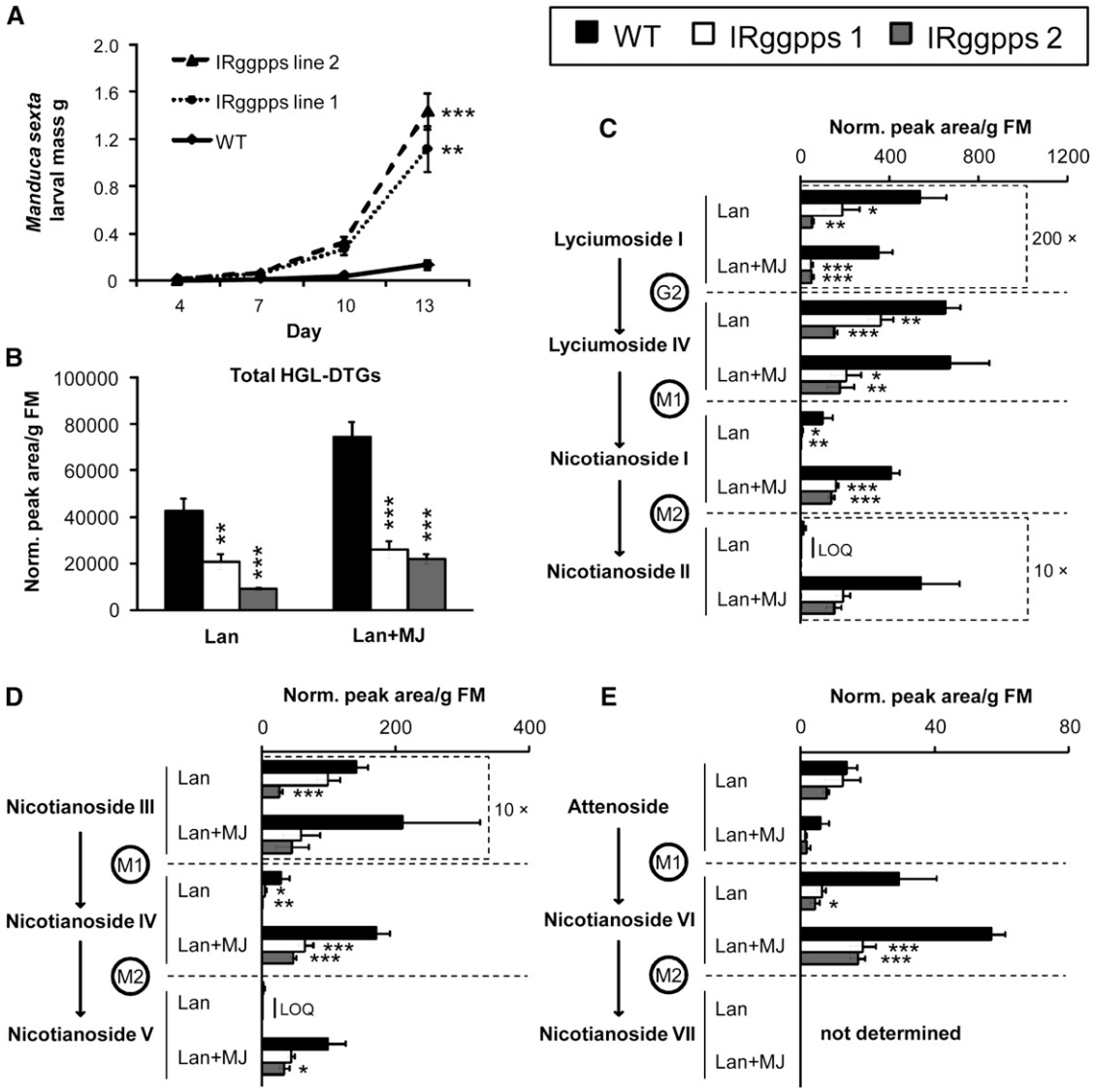

Figure 7. Total HGL-DTGs Have a Significant Effect on the Growth of the Specialist Herbivore *M. sexta*.

(A) Mass of *M. sexta* larvae feeding on two independently silenced IR*ggpps* lines versus the wild type (average ± SE; final $n = 7$ to 15 plants with one larva per plant; see Methods). Larvae grow significantly larger on both lines of IR*ggpps*: growth on IR*ggpps* line 1 was significantly faster by day 4 ($P = 0.018$) and on both IR*ggpps* lines by day 7 (line 1, $P = 0.011$; line 2, $P = 0.016$) as determined by a repeat-measures ANOVA followed by Bonferroni-corrected tests for each day. For clarity, significance is shown only for day 13: ** $P < 0.01$ and *** $P < 0.001$.

(B) to **(E)** Total HGL-DTGs **(B)** and concentrations of individual compounds (**[C]** to **[E]**) in mature young rosette leaves of the wild type and both lines of IR*ggpps* 3 d after treatment with lan or lan+MJ (average + SE). Note that some compounds have been multiplied by constants to fit the scale of the graph and that scales change among graphs.

Asterisks indicate significantly lower levels of HGL-DTGs in IR*ggpps* in one-way ANOVAs within treatment (*$P < 0.05$, ** $P < 0.01$, and *** $P < 0.001$ in Bonferroni-corrected tests). LOQ, below limit of quantification.

plants, albeit from a larger precursor pool, we conclude that JA biosynthesis and perception strongly regulate malonylation, and JA perception accelerates glycosylation (Figure 9). IR*lox3* plants accumulate core compounds either because their residual pool of JAs is sufficient to allow glycosylation, but not malonylation, to proceed at wild-type rates, or because non- JA signaling molecules can interact with COI1 to influence glycosylation.

In wild-type plants, W+OS elicitation reduces concentrations of precursors by 3 d compared with control plants, but lan+MJ treatment does not (Figure 5A), and IR*coi1* plants are unable to produce wild-type levels of total HGL-DTGs (Figure 6A). Thus, JAs also promote the initiation of HGL-DTG biosynthesis, and the precursor pool is maintained at a level corresponding to the magnitude or duration of JA elicitation, presumably to permit

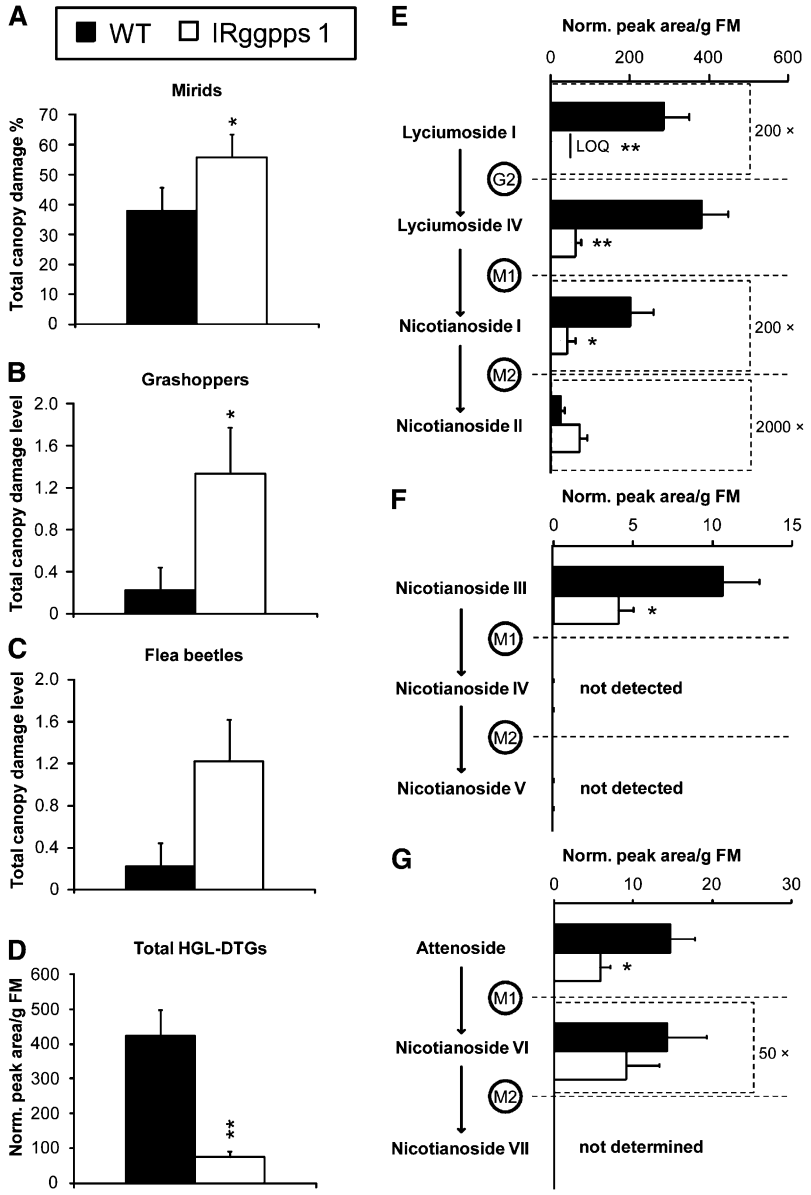

Figure 8. HGL-DTGs Reduce Damage from Generalist Herbivores in Nature.

(A) The most abundant herbivore in the 2008 field season, mirids caused significantly more damage on IR*ggpps* line 1 than on wild-type plants in the field by May 16th (average + SE; $n = 9$ pairs; *P < 0.05 in paired *t* tests).
(B) Grasshoppers caused significantly more damage on IR*ggpps* line 1 by May 16th (average + SE, *P < 0.05 in Wilcoxon's sign-rank test).
(C) Flea beetles tended to cause more damage on IR*ggpps* line 1 at the beginning of damage measurements on May 8th; differences are not statistically significant (average + SE, Wilcoxon's sign-rank test). Scale for less abundant herbivores in **(B)** and **(C)**: damage level 0 = 0% total canopy damage; level 1, <1%; level 2, < 5%; level 3, 5 to 10%.
(D) to **(G)** Total HGL-DTGs **(D)** and concentrations of individual compounds (average + SE; **[E]** to **[G]**) in undamaged systemic leaves harvested from pairs of the wild type and IR*ggpps* line 1 on May 15th. Note that some compounds have been multiplied by constants to fit the scale of the graph and that scales change. *P < 0.05 and ** P < 0.01 in paired *t* tests.
LOQ, below limit of quantification.

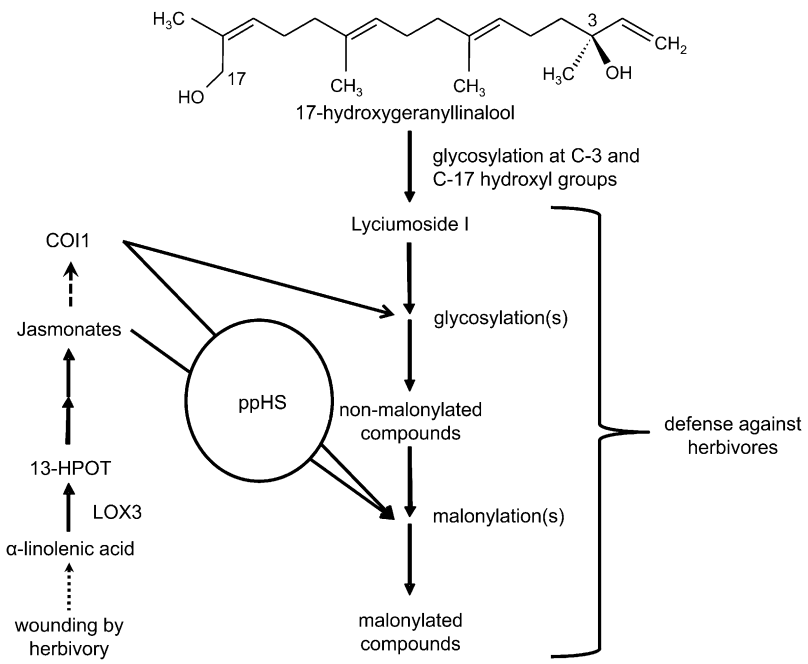

Figure 9. Proposed Model for the Regulation of HGL-DTG Biosynthesis and Effect on Herbivores in *N. attenuata*.

A simplified biosynthetic pathway is shown for HGL-DTGs from the 17-hydroxygeranylinalool skeleton to the higher molecular weight HGL-DTGs and their mono- and dimalonylated forms. Herbivore attack and larval oral secretions (OS) elicits JA biosynthesis (requiring *lox3*) and perception (requiring *coi1*), which strongly regulate malonylation of HGL-DTGs, and JA perception accelerates glycosylation. ppHS may fine-tune JA-mediated malonylation by altering either the perception of JAs or the positive feedback of JAs on their own biosynthesis. The accumulated HGL-DTGs function as a profoundly effective defense against herbivores.

the more rapid biosynthesis of malonylated compounds. Again, we see a parallel to nicotine accumulation: increasing concentrations of JAs correspond to a higher biosynthetic set point for the period after elicitation (Baldwin and Schmelz, 1996; Baldwin, 1996, 1999; Baldwin et al., 1997).

JA Regulation of HGL-DTG Biosynthesis Is Tuned by ppHS

IR*sys* plants tend to accumulate lower levels of malonylated compounds than wild-type plants, and this tendency is significant after lan+MJ treatment for two of three dimalonylated compounds (Figures 5D to 5F). Like IR*coi1*, unelicited IR*sys* plants also accumulate significantly higher concentrations of the precursor lyciumoside I than do wild-type plants, although of the malonylated compounds only nicotianoside VI is significantly lower in unelicited IR*sys* plants (Figures 5D and 5E). Unlike systemin precursor proteins in *L. esculentum*, ppHS overexpression does not enhance herbivore-induced defense responses of *N. attenuata* (Berger and Baldwin, 2007), consistent with the hypothesis that ppHS is involved in tuning, rather than initiating the HGL-DTG biosynthetic cascade. IR*sys* plants do have lower levels of the jasmonoyl Ile conjugate (JA-Ile) in flowers and an altered kinetic of JA accumulation in the leaves: peak levels of JA are no different from wild-type plants, but the increase after herbivore elicitation is not as rapid (Berger and Baldwin, 2007, 2009). This may indicate a role for ppHS in modifying sensitivity to JAs, as has been proposed for systemin in tomato (Ryan and Pearce, 2003). It is tempting to speculate that ppHS may modify JA-mediated malonylation by altering the perception of JAs or the positive feedback of JAs on their own biosynthesis (Figure 9).

Role of Malonylation in HGL-DTG Regulation and Activity

IR*sys* plants are impaired in the accumulation of dimalonylated compounds (Figure 5), which accumulate to the highest levels in wild-type leaves (Figure 2B), but their foliage is not more susceptible to herbivores (Berger and Baldwin, 2007), which indicates that malonylation is not critical for any toxic or deterrent function of HGL-DTGs. Furthermore, we discovered that the malonyl group is easily lost to nonenzymatic cleavage in solutions with a similar pH to the lepidopteran midgut (pH 11; data not shown; Dow, 1992); thus, it is unlikely that malonylated compounds would survive in the midgut. It is unlikely that the loss of the malonyl group would result in a more toxic compound, but rather that cleavage of the sugar moieties and exposure of the geranyllinalool skeleton could be toxic (Lemaire et al., 1990; Snook et al., 1997). We propose that malonyl moieties are more likely involved in regulating within-plant transport and storage of HGL-DTGs.

Malonylation of secondary metabolites, such as flavonoids, isoflavonoids, and anthocyanins, is a common phenomenon in many plant species, among them *Medicago trunculata*, lupins (*Lupinus* spp), and *N. tabacum*, and may alter molecular

properties in several ways: by stabilizing labile structures (Matern et al., 1983; Suzuki et al., 2002), enhancing their solubility in water (Heller and Forkman, 1994), detoxifying xenobiotics (Sandermann, 1991, 1994) and biogenic compounds (Taguchi et al., 2005), preventing the enzymatic degradation of glycoconjugates (Yu et al., 2008), or sequestering compounds to different cellular compartments, including vacuoles and the cell wall (Harborne, 2000; Markham et al., 2000). Malonylation might also activate HGL-DTGs prior to dimer formation: dimeric HGL-DTGs in *C. annuum* can modulate the reorganization of actin filaments and thus change the structure and permeability of tight junctions in human intestinal cells (Hashimoto et al., 1997).

Unlike some phenolic glucosides, malonylated HGL-DTGs are less soluble in water than are core compounds (see Supplemental Figure 1 online; Taguchi et al., 2005), which may permit them to more easily cross membranes, but should impede phloem transport. Morris and Larcombe (1995) used ^{14}C labeling to show that the water-soluble ethylene precursor [2,3-^{14}C]1-aminocyclopropane-1-carboxylic acid was freely transported in the phloem of cotton plants (*Gossypium hirsutum*) and quickly converted to the less-soluble malonyl-[^{14}C]ACC ([^{14}C]MACC) in destination tissues; [^{14}C]MACC did not reenter the phloem, and MACC was not found in phloem exudates. Bouzayen et al. (1989) demonstrated ATP-dependent active transport of MACC into vacuoles isolated from the Madagascar periwinkle (*Catharanthus roseus*) and proposed this as a mechanism for recovering stress-induced amino acid conjugates from the phloem. In senescing leaves, chlorophyll is broken down into fragments, including the linear diterpene alcohol phytol, which has a similar structure to geranyllinalool, and these cleavage products are often found in the vacuole as glycosides or malonyl conjugates (Martinoia et al., 2000). Thus, malonylation likely traps HGL-DTGs in target tissues, perhaps by marking them for transport into vacuoles (Matern et al., 1986).

W+OS-elicited young flowering plants accumulated core rather than malonylated HGL-DTGs in their calyxes (Figure 2B). This could be due to the arrival of core compounds at the calyxes via phloem transport. In fact, although treatment reliably elevated concentrations of malonylated HGL-DTGs across our experiments, relative concentrations of core versus malonylated compounds were highly variable. This variability may be a snapshot of the current status of HGL-DTG import versus export or biosynthesis versus fixation in the tissue sampled. Alternatively, malonylated HGL-DTGs could become substrates for HGL-DTG dimerization (Hashimoto et al., 1997), which would explain the unexpected decrease in concentrations of malonylated attenoside products following lan+MJ elicitation (Figure 5). Further research must determine the role of malonylation in the metabolism and allocation of HGL-DTGs and the extent to which it is important for the function of HGL-DTGs in defending different plant tissues from their attackers.

Ecological Significance and Metabolic Role of HGL-DTGs

HGL-DTGs are biosynthetically classified as secondary metabolites but are present in wild-type leaves in amounts similar to starch (mg/g FM; see Supplemental Figure 2 online), and their regulation is correlated with patterns in primary metabolism: concentrations of all except malonylated HGL-DTGs increased in unelicited plants during the night (14 h, Figure 4), suggesting that HGL-DTG biosynthesis may occur in the dark following daytime photosynthetic fixation, parallel to starch degradation in the plastid and transport of monomeric sugar to the cytosol (Lu et al., 2005). Although the production of sugar and malonyl moieties and the plastid-produced diterpene skeleton of HGL-DTGs are all directly linked to photosynthesis, nothing is known about the role of diurnal rhythms or light in regulating concentrations of individual and total HGL-DTGs. There are seasonal fluctuations in levels of lyciumosides I, II, and III in *L. chinense* (Terauchi et al., 1997a, 1997b), which could be due in part to changing light levels. Further studies must address the separate influences of light, diurnal rhythms, and photosynthetic rates on HGL-DTG biosynthesis, as well as the potential role of HGL-DTGs as a sugar storage form that the plant, but not its enemies, may later draw on for nutrition.

A growing number of metabolites are known to function both in primary metabolism as well as in defense signaling or altering the nutritive value of plant tissue (Schwachtje and Baldwin, 2006, 2008). Some secondary metabolites are thought to be remobilized and degraded for use of the component nutrients in primary metabolism. For example, ammonia or hydrogen cyanide from the breakdown of cyanogenic glycosides in barley (*Hordeum vulgare*), cassava (*Manihot esculenta*), rubber tree (*Hevea brasiliensis*), and sorghum (*Sorghum bicolor*) may provide an important source of nitrogen for germinating seeds and mature plants (Selmar et al., 1988; Forslund and Jonsson, 1997; Siritunga and Sayre, 2004; Jenrich et al., 2007). Moreover, cleavage of cyanogenic glycosides to release benzaldehyde may also act as an indirect defense during aphid feeding (Han and Chen, 2002; Hatano et al., 2008).

JAs are known to regulate primary metabolism as well as the biosynthesis of defense compounds and are linked to primary metabolism via sugar signaling and JA-Ile formation (Creelman and Mullet, 1997; Schwachtje and Baldwin, 2008). Likewise, systemin and systemin-like precursor proteins regulate growth and development as well as JA-mediated defense (Berger and Baldwin, 2009; Schmidt and Baldwin, 2009). Thus, the regulation of malonylation by JAs and ppHS could reflect the original importance of malonylated HGL-DTGs in primary or secondary metabolism, or both.

A 50 to 75% reduction of total HGL-DTGs in IR*ggpps* lines corresponded to a tremendous increase in *M. sexta* growth and to increased damage by native generalist herbivores in a natural habitat (Figures 7 and 8). Although silencing a GGPPS gene has the potential to reduce levels of other diterpenoid derivatives, growth and defensive metabolite data from glasshouse and field-grown plants (Figures 7 and 8; see Supplemental Figures 4 to 7 online) show that the main difference between IR*ggpps* and wild-type plants during the time over which we conducted bioassays was the level of HGL-DTGs. Data from a competition assay in the glasshouse (see Supplemental Figure 4 online) confirm that IR*ggpps* plants grow normally and do not suffer a reduction in seed production under glasshouse conditions, implying that there is no strong effect of silencing *ggpps* on primary metabolism. This is consistent with results from Jassbi et al. (2008) that showed that there was no effect on carotenoid content from the

transient silencing of *ggpps* using VIGS, in contrast with the complete photobleaching that is observed after VIGS of *N. attenuata* phytoene desaturase (Saedler and Baldwin, 2004). They concluded that *ggpps* is one of multiple GGPPS enzymes in *N. attenuata* and that it provides substrate mainly for HGL-DTGs. Furthermore, silencing *ggpps* does not lead to the accumulation of any toxic compounds, and although it could increase flux to other areas of terpenoid metabolism, we have not seen evidence that this occurs (e.g., levels of terpenoid volatiles were not elevated in IR*ggpps* plants grown under normal glasshouse conditions). Finally, Jassbi et al. (2008) found no evidence of other diterpenoid secondary metabolites that might be formed from GGPP, including the cembrane- and labdane-type diterpenoids found in *N. tabacum*. Thus, *ggpps* silencing is an effective tool for investigating the role of HGL-DTGs in *N. attenuata*.

Differences in naturally occurring levels of HGL-DTGs are known to be directly correlated with differences in resistance against herbivores for *N. attenuata* and *N. tabacum* (Snook et al., 1997; Mitra et al., 2008), and transient silencing of *ggpps* had a greater positive effect on *M. sexta* larval growth than did reducing nicotine or TPIs and did not influence the levels of nontarget diterpenes such as chlorophyll (Jassbi et al., 2008). It is clear that HGL-DTGs contribute substantially to defense in *Nicotiana* spp. By contrast, it is entirely unclear what role, if any, malonylation plays in the defensive function of HGL-DTGs and why it is apparently the most regulated step in HGL-DTG biosynthesis. Determining the effect of malonylation on the properties and distribution of HGL-DTGs will be critical to understanding their function in plants.

METHODS

Plant Material and Growth Conditions

Seed germination, glasshouse growth conditions, and the *Agrobacterium tumefaciens* (strain LBA 4404)–mediated transformation procedure are described by Krügel et al. (2002). Seeds of the 30th generation of an inbred line of *Nicotiana attenuata* Torr. Ex Watts were used as the wild-type plant in all experiments. For the field experiment, seedlings were transferred to 50-mm peat pellets (Jiffy) 15 d after germination and gradually hardened to the environmental conditions of high sun exposure and low relative humidity over 2 weeks. Small, adapted, rosette-stage plants of equal size were transplanted into a field plot in a native habitat in Utah and watered daily for 2 weeks until roots were established.

The *A. tumefaciens* (strain LBA 4404)–mediated transformation procedure is described by Krügel et al. (2002). To determine the role of JA and systemin signaling in HGL-DTG elicitation, we used the inverted repeat RNAi transformants IR*coi1* (Paschold et al., 2007), IR*lox3* (inverted repeat construct created with a 467-bp segment of the Na *lox3* fragment used in Krügel et al., 2002 to create the antisense as-*lox* plants characterized in Halitschke and Baldwin, 2003), and IR*sys* (Berger and Baldwin, 2007). To determine the role of total GGPPS products in defense against herbivores, we used two independently transformed RNAi lines (IR*ggpps* lines 1 and 2) containing an inverted repeat construct generated from a unique fragment comprising positions 506 to 823 of the *Na ggpps* sequence (primers are in Jassbi et al., 2008; see Supplemental Table 1 online). Vector construction and the pRESC5 plasmid are described by Steppuhn et al. (2004). Homozygosity of T2 plants was determined by screening for resistance to hygromycin (hygromycin phosphotransferase II gene from pCAMBIA-1301contained in the pRESC5 vector).

Two independently transformed lines were chosen for further characterization based on high constitutive silencing efficiency of *ggpps* and similar metabolite production, growth, and morphology to wild-type plants (see Supplemental Figures 4 and 5 online). Transcript accumulation was determined by TaqMan qPCR as described by Wu et al. (2007) with primers GGPPS F1 (5′-CCAAAACTGCTGGGATTGGA-3′) and GGPPS R1 (5′-CAGCTGTTGTTTAGCATCTCG-3′) and probe GGPPS P1 (5′-AGGCTAAGGAATTTGCGGCGGAGCT-3′) designed from positions 966 to 1019 of the *ggpps* sequence using Primer Express v1.5 from Applied Biosystems. Expression was quantified relative to that of *N. attenuata actin* using primers Actin F1 (5′-GGTCGTACCACCGGTATTGTG-3′) and Actin F2 (5′-GTCAAGACGGAGAATGGCATG-3′) with probe Actin P1 (5′-TCAGCCACACCGTCCCAATTTATGAGG-3′). Flow cytometric analysis as described by Bubner et al. (2006) confirmed that both lines were diploid. Growth and fitness were measured in a competition experiment where one IR*ggpps* line 1 plant was paired with one empty vector plant in a 2-liter pot (pRESC empty vector characterized in Schwachtje et al., 2008); beginning on day 33 after germination, the two plants in a pot were elicited one time/week either with Lan or Lan+MJ (n = 10 pairs) to the leaf one older than the source/sink transition leaf (+1) on rosette-stage and bolting plants or to the base of the stem on elongated plants. The +1 leaf on 10 35-d-old rosette plants/line was elicited either with lan or lan+MJ (n = 5 plants) as described below and harvested after 3 d for analysis of HGL-DTGs and other metabolites involved in defense against herbivores (nicotine and TPI) and UV tolerance (rutin and chlorogenic acid). Nicotine, chlorogenic acid, and rutin were analyzed on an Agilent HPLC system according to Keinänen et al. (2001); TPI activity levels were determined by radial diffusion assay as described by Van Dam et al. (2001); determination of HGL-DTG concentrations is described below.

Growth of line 1 was also compared with the wild type in the field: maximum rosette diameter and stalk elongation were measured on the 6th, 8th, 15th, and 21st of May from before the rosette was fully developed through the onset of flowering. Growth was always measured after arthropod presence and herbivore damage had been recorded. One undamaged or minimally damaged green leaf per plant was collected from field-grown IR*ggpps* line 1 and wild type on May 16th (when herbivore attack was at its highest), extracted, and analyzed for levels of HGL-DTGs and other secondary metabolites as described above; harvested leaf positions were similar within pairs.

Purification of HGL-DTGs

Leaf material was ground in liquid nitrogen and was split into ~200-mg aliquots. Each aliquot was extracted in 1 mL extracting solution (40% methanol and 0.05% formic acid) with 900 mg lysing matrix (BIO 101; Qbiogen) by shaking twice at 6.5 ms^{-1} for 20 s (FastPrep FP 120; Thermo Savant). Homogenized samples were centrifuged at 16,000*g* for 20 min at 4°C. Supernatants were pooled in a round flask and evaporated in a rotary evaporator to one-fourth of the original volume. The supernatant was centrifuged again at 16,000*g* for 3 min at 4°C. The concentrated solution was fractionated on a reverse-phase HPLC [Luna C-18 (2), 250 × 10 mm; Phenomenex] at a 2 mL/min flow rate. Mixtures of two solvents were used to elute analytes from the column: A (Millipore water, 0.1% acetonitrile, and 0.05% formic acid) and B (acetonitrile and 0.05% formic acid). HPLC-grade acetonitrile was purchased from Malinckrodt Baker, formic acid was purchased from Fluka, and ultrapure water was obtained using a Millipore model Milli-Q Advantage A10. Sample elution steps were as follows: 0 to 2 min, 0% of B, 2 to 25 min, 0 to 70% of B, 25 to 27 min, 70% of B, 27 to 35 min, 70 to 98% of B, 35 to 37 min, 98% of B, 37 to 40 min, 98 to 0% of B. Nearly pure nicotianosides I, II, and III and lyciumoside I were collected from fractions 40 to 48. Fractions were passed through an Oasis C-18 cartridge (Waters) to remove formic acid. Extracts were then

evaporated completely in a vacuum concentrator (3.7 mbar; Concentrator 5301; Eppendorf).

Structural Determination by NMR Spectroscopy

The 1H and 13C NMR spectra were determined on a Bruker Avance AV-500 NMR spectrometer at 500 and 125 MHz.

HGL-DTG Quantification in Plant Tissues

Buffer A consisted of 60% solution 1 (2.3 mL/L of acetic acid, 3.41 g/L ammonium acetate adjusted to pH 4.8 with 1 M NH_4OH) and 40% methanol. Buffer B consisted of Buffer A (10%) and 40% methanol (90%). HGL-DTGs were extracted from plant material in 1 mL Buffer A spiked with the following internal standards (Buffer A + ISTDs): 600 ng/mL reserpine (Spectrum Laboratory), 10,000 ng/mL 9, 10-dihydro-dideuteriojasmonic acid (^{2}D-JA), 200 ng/mL atropine (Fluka), and 1000 ng/mL glycyrrhizinic acid (Sigma-Aldrich).

Plant tissue samples were flash-frozen in liquid nitrogen and stored at −80°C until extraction. Samples were ground in liquid nitrogen, and ~100 mg aliquots (mass was recorded and later used for normalization) were extracted in 1 mL Buffer A + ISTDs with 900 mg lysing matrix by homogenization twice at 6.5 ms^{-1} for 45 s (FastPrep FP 120 Thermo Savant). Homogenized samples were centrifuged at 16,000*g* for 20 min at 4°C. Supernatants were removed and again centrifuged at 16,000*g* for 20 min at 4°C. Particle-free supernatants were diluted 1:50 with Buffer B for HPLC–tandem mass spectrometry analysis.

Ten microliters of undiluted, particle-free extract was analyzed by reverse-phase HPLC coupled to a Varian 1200-liters triple-quad mass spectrometry (MS/MS/MS) system. HPLC separation was achieved using a ProntoSIL UHC-520 (50 × 2.0 mm) (BISCHOFF Analysentechnik undgeräte), with a mobile phase flow rate of 0.2 mL/min. The mobile phase was a gradient of A (water, 0.1% acetonitrile, and 0.05% formic acid) and B (acetonitrile and 0.05% formic acid) starting at 20% B and rising linearly to 70% over 3.5 min. The gradient was held at 70% B for 7.5 min, followed by reequilibration for 3.5 min. Multiple reaction monitoring was conducted on parent-ion/daughter-ion selections after negative ionization: 213/59 (D2-JA), 629.4/467.4 (lyciumoside I), 775.4/629.4 (lyciumoside IV), 791.4/629.4 (lyciumoside II), 821.4/351.4 (glycyrrhizinic acid), 861.4/758.4 (nicotianoside I), 921.4/775.4 (nicotianoside III), 937.4/791.4 (attenoside), 947.4/859.4 (nicotianoside II), 1007.5/963.5 (nicotianoside IV), 1023.47/979.46 (nicotianoside VI), 1093.5/1005.5 (nicotianoside V), and 1109.5/979.46 (nicotianoside VII). The area beneath the multiple reaction monitoring product ion peak was recorded for detected analytes and ISTDs using the operating software from Varian (MS Workstation).

Concentrations of individual compounds were calculated in normalized peak area (PA) per g FM as $(PA_{compound})/(PA_{glycyrrhizinic\ acid} * FM_{extracted})$. Classes of HGL-DTGs per tissue type (e.g., total malonylated compounds) were calculated as $\Sigma(PA_{compound}/PA_{glycyrrhizinic\ acid})/FM_{extracted}$. These concentrations were multiplied by the average FM of each tissue type to calculate total HGL-DTGs per tissue.

HPLC/Time-of-Flight Mass Spectrometry

Samples were extracted as above, and the same solvents (A and B) were used for separation. HPLC was performed using an Agilent HPLC 1100 Series system, combined with an Phenomenex Gemini NX 3u (150 × 2.0 mm) column. Sample elution steps were as follows: 0 to 2 min isocratic at 5% B, 2 to 30 min linear gradient up to 80% of B, 30 to 35 min isocratic at 80% of B, followed by a return to starting conditions and column equilibration steps. The injection volume was 2 μL and the flow rate 0.2 mL/min.

Mass spectrometry was performed using a Bruker microTOF (Bruker Daltonics) time-of-flight mass spectrometer with an electrospray ionization source operating both in positive and in negative ion mode. Electrospray ionization conditions: TOF 2100 V, capillary voltage 4500 V, capillary exit 130 V, dry temperature 200°C, dry gas flow of 8 l/min. Mass calibration was performed using sodium formiate (50 mL isopropanol, 200 μL formic acid, and 1 mL 1 M NaOH in water). Compounds and types of compounds in samples were quantified as described above.

Ontogeny of HGL-DTG Accumulation

To determine the within-plant dynamics of HGL-DTGs in plants of different ages, one mature, green leaf per plant on 34-d-old rosette, 44-d-old elongated, 54-d-old flowering, and 68-d-old flowering-stage plants was wounded with a pattern wheel to produce three rows of holes on each side of the midvein, and 50 μL of *Manduca sexta* oral secretions diluted 1:5 with distilled water (OS) was applied to the wounds by gently rubbing the pipetted liquid across the leaf surface using a gloved finger (W+OS) (n = 4 plants). All tissue types were harvested from elicited and control plants (n = 4) after 3 d. Depending on the developmental stage, harvested tissues from the same plant were pooled into the following groups: ripe seed capsules, unripe seed capsules, flowers, calyxes, buds, small stem leaves (on side stems), large stem leaves (on the main stem), young rosette leaves (still green), senescing rosette leaves, and senescent rosette leaves (completely yellow). The stem and the elicited leaf or the equivalent leaf position on control plants were harvested separately. During the harvest, control plants were alternated with W+OS-elicited plants, and growth stages were alternated, so that the harvesting of all treatments and growth stages was distributed throughout the entire harvesting period. Samples were flash-frozen in liquid nitrogen and then stored at −80°C until use.

HGL-DTGs were extracted from each tissue type of each growth stage as described above. We harvested and weighed the total tissues of each type (FM) from separate, unelicited plants of the same four growth stages (n = 5 plants), and the total mass of each tissue was used to calculate the allometric distribution of HGL-DTGs (total amount in each tissue type) based on concentrations measured in each tissue. We built a mixed linear model that used the total HGL-DTGs in each tissue sample from a particular growth stage to estimate the average total HGL-DTG contents of the whole plant at each growth stage with a calculated standard error using R package lme4 (R-Project; http://www.r-project.org).

RNA from separate, unelicited 54-d-old wild-type plants (n = 4) was used to analyze *ggpps* transcripts in different tissues. Synthesis of cDNA from 0.5 μg of RNA per sample and TaqMan (Applied Biosystems) quantitative PCR were conducted as described above.

Dynamics of HGL-DTGs after Simulated Herbivory

In order to analyze the dynamics of different HGL-DTGs after herbivore attack, five leaves per plant on 30-d-old rosette-stage plants were wounded with a pattern wheel to produce three rows of holes on each side of the midvein, and 20 μL of OS was applied to the wounds (W+OS) as described in the previous section. Leaves at the elicited positions were harvested from elicited and unelicited (control) plants at 1, 4, 14, and 72 h, and 5 and 7 d after elicitation (n = 5 plants/treatment/time point). All five elicited leaves, or the equivalent leaves on control plants, were pooled together for each individual plant prior to extraction, but samples were not pooled among plants. Samples were flash-frozen in liquid nitrogen and then stored at −80°C until use. HGL-DTGs were extracted and quantified.

JA and Systemin Signaling in HGL-DTG Biosynthesis

To determine the role of jasmonate biosynthesis and perception in the elicitation of different HGL-DTGs in *N. attenuata*, the oldest stem leaves

(S1) of 44-d-old elongated IR*lox3*, IR*coi1*, and wild-type plants received one of three treatments. To simulate herbivory, leaves on five plants/line were elicited with W+OS using 20 μL of OS, and to supplement JAs, another five plants/line were elicited with either with 20 μL of lanolin paste containing 150 μg lan+MJ (Lan+MJ) or with 20 μL of lanolin (Lan). Elicited leaves and S1 leaves from unelicited (control) plants were harvested after 3 d and flash-frozen in liquid nitrogen, then stored at −80°C until use. Plants impaired in systemin-mediated signaling (IR*sys*) were compared with wild-type plants in a second experiment using identical methods. HGL-DTGs were extracted and quantified.

Effect of HGL-DTGs on the Specialist M. sexta

Wild-type plants and plants of both lines of IR*ggpps* were grown in the glasshouse in Jena as described above. *M. sexta* eggs were taken from our own colony. One *M. sexta* neonate was placed on the S1 leaf of each plant. The 39-d-old bolting plants (n = 23 plants) from both lines of IR*ggpps* and the wild type were used. Larval mass was determined on days 4, 7, 10, and 13, by which time larvae were in the 3rd to 4th instar. Due to mortality and to larval movement off the plants, replicate number decreased during the assay: by day 13, seven larvae remained on the wild type, 15 on IR*ggpps* line 1, and 13 on IR*ggpps* line 2. Plants were randomized spatially on the same table in the greenhouse, and placement and weighing of larvae were also randomized among genotypes.

Field Bioassays

Ten replicates consisting of pairs of wild-type and IR*ggpps* line 1 plants were transplanted on April 21, 2008 into a field plot within a natural *N. attenuata* habitat on Lytle Ranch near Santa Clara, Utah, under Animal and Plant Health Inspection Service notification number 06-242-3r, as described above.

Presence of arthropod herbivores and predators and leaf area damage as percentage of canopy damaged by herbivores were monitored on May 6th, 8th, 12th, and 16th. Small amounts of damage were estimated using categories: 0%, <1%, <5%, and 5 to 10%; larger amounts of damage were estimated to the nearest 5% of total canopy area. Pairwise comparisons allowed even small differences in canopy damage to be accurately assessed within pairs, although the absolute percentage of canopy damage was not measured with the same accuracy. Characteristic damage caused by Noctuidae larvae (*Spodoptera* spp), flea beetles (*Epitrix hirtipennis* Melsheimer and *Epitrix subcrinita* Le Conte), grasshoppers (*Trimerotropis* spp), mirids (*Tupiocoris notatus* Distant), and leaf miners or due to mechanical damage was recorded separately.

Field data cited for IR*sys* lines comes from 14 pairs of IR*sys* and wild type planted into the same field plot in 2006 (Berger and Baldwin, 2007).

Statistical Analysis

Data were analyzed with Excel (Microsoft), SPSS 17.0, StatView 5.0 (SAS Institute), or R (R-Project; http://www.r-project.org). When necessary, data were log transformed to meet requirements for homogeneity of variance: raw values were augmented by 1 to include any zero values, and the resulting values were log2 transformed. Unless otherwise stated, parametric data were compared using ANOVAs followed by Bonferroni post-hoc tests or Student's t tests with Ps altered as necessary for multiple comparisons using the Bonferroni correction. Larval mass in the glasshouse bioassay was analyzed by a repeat-measures ANOVA followed by Bonferroni post-hoc tests on individual days. Paired t tests were used for field data. If variance was not homogeneous following transformation, data were compared via Kruskal-Wallis (multiple comparisons) or either Wilcoxon signed-rank or Welch (t test) tests.

Accession Numbers

Sequence data from this article can be found in the GenBank/EMBL data libraries under the following accession numbers: hygromycin phosphotransferase II from pCAMBIA-1301 complete gene sequence (used in the pRESC5 vector), AF234297; Na *ggpps* complete cDNA, EF382626; *N. attenuata actin* (used as an internal standard in TaqMan [Applied Biosystems] quantitative PCR analysis), EU273278.

Supplemental Data

The following materials are available in the online version of this article:

Supplemental Figure 1. Optimization of Buffer Composition for Extraction of HGL-DTGs from *N. attenuata* Leaves.

Supplemental Figure 2. Standard Addition Curve for Mass Spectrometry Measurements and Calculated Quantities of HGL-DTGs in Leaf Tissue.

Supplemental Figure 3. Effects of Methyl Jasmonate Application on HGL-DTG Biosynthesis in Wild-Type Plants and Plants Impaired in Jasmonate Biosynthesis (IR*lox3*) and Perception (IR*coi1*) or ppHS Signaling (IR*sys*).

Supplemental Figure 4. Growth and Fitness of Empty Vector and IR*ggpps* Line 1 Plants in a Competition Experiment in the Glasshouse.

Supplemental Figure 5. Silencing Efficiency and Secondary Metabolites in IR*ggpps* Lines versus the Wild Type.

Supplemental Figure 6. Secondary Metabolites in Wild-Type and IR*ggpps* Line 1 Plants Grown in a Paired Field Plot Experiment in *N. attenuata*'s Native Habitat.

Supplemental Figure 7. Growth and Morphology of Wild-Type and IR*ggpps* Line 1 Plants Grown in a Paired Field Plot Experiment in *N. attenuata*'s Native Habitat.

Supplemental Table 1. Mass Spectral Assignments and NMR Spectra of HGL-DTGs in *N. attenuata*.

Supplemental Table 2. Mass Spectral Data for All HGL-DTGs Measured in *N. attenuata*.

Supplemental Table 3. Results of Student's t Tests Comparing Individual HGL-DTGs at Several Time Points in Rosette Control Leaves or Leaves Elicited with Wounding and *Manduca sexta* Oral Secretions (W+OS).

Supplemental Table 4. Results of ANOVAs Comparing Individual HGL-DTGs in IR*lox3*, IR*coi1*, or IR*sys* Plants after Different Treatments.

Supplemental Table 5. Results of ANOVAs Comparing Individual HGL-DTGs in Wild-Type Leaves After Different Treatments.

Supplemental Table 6. Results of ANOVAs Comparing Individual HGL-DTGs in the Wild Type versus IR*lox3* and IR*coi1* Leaves.

Supplemental Table 7. Results of Student's t tests Comparing Individual HGL-DTGs in the Wild Type versus IR*sys* Leaves.

Supplemental Table 8. Results of ANOVAs Comparing Individual HGL-DTGs in the Wild Type versus IR*ggpps* Lines 1 and 2.

Supplemental Table 9. Results of Paired t tests Comparing Growth and Fitness Measurements in IRggpps Line 1 and Empty Vector Control Plants Grown in Competition with Lan or Lan+MJ Treatment.

ACKNOWLEDGMENTS

We thank the gardening staff at the Max Planck Institute for Chemical Ecology and the 2008 field crew, in particular Celia Diezel and Danny

Kessler, for plant growth and care, and Christiane Schubert, Tim Sehrt, and Richard Golnik for help with harvesting and processing samples. We also thank Jens Schumacher, Nicolas Heinzel, and Emmanuel Gaquerel for analytical and statistical advice. Thanks go as well to Brigham Young University for the use of their awesome field station, the Animal and Plant Health Inspection Service for careful regulatory oversight, and the Max Planck Society and the International Max Planck Research School on the Exploration of Ecological Interactions with Chemical and Molecular Techniques for financial support.

Received September 16, 2009; revised December 11, 2009; accepted December 20, 2009; published January 15, 2010.

REFERENCES

Baldwin, I.T. (1996). Allometric limits to the induced accumulation of nicotine in wild tobacco. Plant Species Biol. **11:** 107–114.

Baldwin, I.T. (1999). Inducible nicotine production in native *Nicotiana* as an example of adaptive phenotypic plasticity. J. Chem. Ecol. **25:** 3–30.

Baldwin, I.T., and Schmelz, E.A. (1996). Immunological "memory" in the induced accumulation of nicotine in wild tobacco. Ecology **77:** 236–246.

Baldwin, I.T., Zhang, Z.-P., Diab, N., Ohnmeiss, T.E., McCloud, E.S., Lynds, G.Y., and Schmelz, E.A. (1997). Quantification, correlations and manipulations of wound-induced changes in jasmonic acid and nicotine in *Nicotiana sylvestris.* Planta **201:** 397–404.

Berger, B., and Baldwin, I.T. (2007). The hydroxyproline-rich glycopeptide systemin precursor *Na*preproHypSys does not play a central role in *Nicotiana attenuata*´s anti-herbivore defense responses. Plant Cell Environ. **30:** 1450–1464.

Berger, B., and Baldwin, I.T. (2009). Silencing the hydroxyproline-rich glycopeptide systemin precursor in two accessions of *Nicotiana attenuata* alters flower morphology and rates of self-pollination. Plant Physiol. **149:** 1690–1700.

Bouzayen, M., Latché, A., Pech, J., and Marigo, G. (1989). Carrier-mediated uptake of 1-(malonylamino)cyclopropane-1-carboxylic acid in vacuoles isolated from *Catharanthus roseus* cells. Plant Physiol. **91:** 1317–1322.

Bubner, B., Gase, K., Berger, B., Link, D., and Baldwin, I.T. (2006). Occurrence of tetraploidy in Nicotiana attenuata plants after Agrobacterium-mediated transformation is genotype specific but independent of polysomaty of explant tissue. Plant Cell Rep. **25:** 668–675.

Chini, A., Fonseca, S., Fernández, G., Adie, B., Chico, J.M., Lorenzo, O., Garcia-Casado, G., Lopez-Vidriero, I., Lozano, F.M., Ponce, M. R., Micol, J.L., and Solano, R. (2007). The JAZ family of repressors is the missing link in jasmonate signaling. Nature **448:** 666–671.

Chung, H.S., Koo, A.J.K., Gao, X., Jayanty, S., Thines, B., Jones, A. D., and Howe, G.A. (2008). Regulation and function of *Arabidopsis JASMONATE ZIM*-domain genes in response to wounding and herbivory. Plant Physiol. **146:** 952–964.

Creelman, R.A., and Mullet, J.E. (1997). Biosynthesis and action of jasmonates in plants. Annu. Rev. Plant Physiol. Plant Mol. Biol. **48:** 355–381.

De Marino, S., Borbone, N., Gala, F., Zollo, F., Fico, G., Pagiotti, R., and Iorizzi, M. (2006). New constituents of sweet *Capsicum annuum* L. fruits and evaluation of their biological activity. J. Agric. Food Chem. **54:** 7508–7516.

Dewick, P.M. (2002). The biosynthesis of C_5-C_{25} terpenoid compounds. Nat. Prod. Rep. **19:** 181–222.

Dow, J.A. (1992). pH gradients in lepidopteran midgut. J. Exp. Bot. **172:** 355–375.

Ellis, C., and Turner, J.G. (2002). A conditionally fertile *coi1* allele indicates cross-talk between plant hormone signaling pathways in *Arabidopsis thaliana* seeds and young seedlings. Planta **215:** 549–556.

Forslund, K., and Jonsson, L. (1997). Cyanogenic glycosides and their metabolic enzymes in barley, in relation to nitrogen levels. Physiol. Plant. **101:** 367–372.

Gregersen, S., Jeppesen, P.B., Holst, J.J., and Hermansen, K. (2004). Antihyperglycemic effects of stevioside in type 2 diabetic subjects. Metabolism **53:** 73–75.

Guo, Z., and Wagner, G.J. (1995). Biosynthesis of cembratrienols in cell-free extracts from trichomes of *Nicotiana tabacum.* Plant Sci. **110:** 1–10.

Halitschke, R., and Baldwin, I.T. (2003). Antisense LOX expression increases herbivore performance by decreasing defense responses and inhibiting growth-related transcriptional reorganization in *Nicotiana attenuata.* Plant J. **36:** 794–807.

Han, B.Y., and Chen, Z.M. (2002). Composition of the volatiles from intact and mechanically pierced tea aphid−tea shoot complexes and their attraction to natural enemies of the tea aphid. J. Agric. Food Chem. **50:** 2571–2575.

Hanson, J.R., and De Oliveira, B.H. (1993). Stevioside and related sweet diterpene glycosides. Nat. Prod. Rep. **10:** 301–309.

Harborne, J.B. (2000). Advances in flavonoid research since 1992. Phytochemistry **55:** 481–504.

Hashimoto, K., Kawagishi, H., Nakayama, T., and Shimizu, M. (1997). Effect of capsianoside, a diterpene glycoside, on tight-junctional permeability. Biochim. Biophys. Acta **1323:** 281–290.

Hatano, E., Kunert, G., Michaud, J.P., and Weisser, W.W. (2008). Chemical cues mediating aphid location by natural enemies. Eur. J. Entomol. **105:** 797–806.

Heller, W., and Forkman, G. (1994). In The Flavonoids: Advances in Research Since 1986, J.B. Harborne, ed, (London: Chapman & Hall, pp. 499–535.

Ishii, E.L., Schwab, A.J., and Bracht, A. (1987). Inhibition of monosaccharide transport in the intact rat liver by stevioside. Biochem. Pharmacol. **36:** 1417–1433.

Izumitani, Y., Yahara, S., and Nohara, T. (1990). Novel acyclic diterpene glycosides, capsianosides A-F and I–V from *Capsicum* plants (Solanaceous Studies. XVI). Chem. Pharm. Bull. (Tokyo) **38:** 1299–1307.

Jassbi, A.R., Gase, K., Hettenhausen, C., Schmidt, A., and Baldwin, I.T. (2008). Silencing geranylgeranyl diphosphate synthase in *Nicotiana attenuata* dramatically impairs resistance to *Manduca sexta.* Plant Physiol. **146:** 974–986.

Jassbi, A.R., Zamanizadehnajari, S., Kessler, D., and Baldwin, I.T. (2006). A new acyclic diterpene glycoside from *Nicotiana attenuata* with a mild deterrent effect on feeding *Manduca sexta* larvae. Z. Naturforsch. C **61b:** 1138–1142.

Jenrich, R., Trompetter, I., Bak, S., Olsen, C.E., Moller, B.L., and Piotrowski, M. (2007). Evolution of heteromeric nitrilase complexes in Poaceae with new functions in nitrile metabolism. Proc. Natl. Acad. Sci. USA **104:** 18848–18853.

Keinänen, M., Oldham, N.J., and Baldwin, I.T. (2001). Rapid HPLC screening of jasmonate-induced increases in tobacco alkaloids, phenolics, and diterpene glycosides in *Nicotiana attenuata.* J. Agric. Food Chem. **49:** 3553–3558.

Kessler, A., Halitschke, R., and Baldwin, I.T. (2004). Silencing the jasmonate cascade: Induced plant defenses and insect populations. Science **305:** 665–668.

Kim, N.C., and Kinghorn, A.D. (2002). Highly sweet compounds of plant origin. Arch. Pharm. Res. **25:** 725–746.

Krügel, T., Lim, M., Gase, K., Halitschke, R., and Baldwin, I.T. (2002).

Agrobacterium-mediated transformation of *Nicotiana attenuata*, a model ecological expression system. Chemoecology **12:** 177–183.

Lee, J.-H., Kiyota, N., Ikeda, T., and Nohara, T. (2006). Acyclic diterpene glycosides, capsianosides VIII, IX, X, XIII, XV and XVI from the fruits of paprika *Capsicum annuum* L. var. *grossum* Bailey and jalapeno *Capsicum annuum* L. var. *annuum.* Chem. Pharm. Bull. (Tokyo) **54:** 1365–1369.

Lee, J.-H., Kiyota, N., Ikeda, T., and Nohara, T. (2007). Acyclic diterpene glycosides, capsianosides C, D, E, F and III, from the fruits of hot red pepper *Capsicum annuum* L. used in Kimchi and their revised structures. Chem. Pharm. Bull. (Tokyo) **55:** 1151–1156.

Lee, J.-H., Kiyota, N., Ikeda, T., and Nohara, T. (2008). Three new acyclic diterpene glycosides from the aerial parts of paprika and pimiento. Chem. Pharm. Bull. (Tokyo) **56:** 582–584.

Lemaire, M., Nagnan, P., Clement, J.-L., Lange, C., Peru, L., and Basselier, J.-J. (1990). Geranyllinalool (diterpene alcohol): An insecticidal component of pine wood and termites (Isoptera: *Rhinotermitidae*) in four European ecosystems. J. Chem. Ecol. **16:** 2067–2079.

Li, L., Zhao, Y., McCraig, B.C., Wingerd, B.A., Wang, J., Whalon, M. E., Pichersky, E., and Howe, G.A. (2004). The tomato homolog of CORONATINE-INSENSITIVE1 is required for the maternal control of seed maturation, jasmonate-signaled defense responses, and glandular trichome development. Plant Cell **16:** 126–143.

Lichtenthaler, H. (1999). The 1-deoxy-D-xylulose-5-phosphate pathway of isoprenoid biosynthesis in plants. Annu. Rev. Plant Physiol. Plant Mol. Biol. **50:** 47–65.

Lin, Y., and Wagner, G.J. (1994). Surface disposition and stability of pest-interactive, trichome-exuded diterpenes and sucrose esters of tobacco. J. Chem. Ecol. **20:** 1907–1921.

Lorenzo, O., and Solano, R. (2005). Molecular players regulating the jasmonate signaling network. Plant Biol. **8:** 532–540.

Lou, Y., and Baldwin, I.T. (2003). *Manduca sexta* recognition and resistance among allopolyploid *Nicotiana* host plants. Proc. Natl. Acad. Sci. USA **100:** 14581–14586.

Lu, Y., Gehan, J.P., and Sharkey, T.D. (2005). Daylength and circadian effects on starch degradation and maltose metabolism. Plant Physiol. **138:** 2280–2291.

Marham, K.R., Ryan, K.G., Gould, K.S., and Richards, G.K. (2000). Cell wall sited flavonoids in lisianthus flower petals. Phytochemistry **54:** 681–687.

Martinoia, E., Massonneau, A., and Frangne, N. (2000). Transport processes of solutes across the vacuolar membrane of higher plants. Plant Cell Physiol. **41:** 1175–1186.

Matern, U., Heller, W., and Himmelspach, K. (1983). Conformational changes of apigenin 7-O-(6-O-malonylglucoside), a vacuolar pigment from parsley, with solvent composition and proton concentration. Eur. J. Biochem. **133:** 439–448.

Matern, U., Reichenbach, C., and Heller, W. (1986). Efficient uptake of flavonoids into parsley (Petroselinum hortense) vacuoles requires acylated glycosides. Planta **167:** 183–189.

McKey, D. (1979). The distribution of secondary compounds within plants. In Herbivores: Their Interaction with Secondary Plant Metabolites. G. Rosenthal and D. Janzen, eds (New York: Academic Press), pp. 55–133.

Mewis, I., Appel, H.M., Hom, A., Raina, R., and Schultz, J.C. (2005). Major signaling pathways modulate *Arabidopsis* glucosinolate accumulation and response to both phloem-feeding and chewing insects. Plant Physiol. **138:** 1149–1162.

Mitra, S., Wünsche, H., Giri, A., Hivrale, V., and Baldwin, I.T. (2008). Silencing 7 herbivory-regulated proteins in *Nicotiana attenuata* to understand their function in plant–herbivore interactions. Funct. Ecol. **22:** 606–615.

Morris, D.A., and Larcombe, N.J. (1995). Phloem transport and conjugation of foliar-applied 1-aminocyclopropane-1-carboxylic acid in cotton (*Gossypium hirsutum* L.). J. Plant Physiol. **146:** 429–436.

Mueller, M.J., Brodschelm, W., Spannagl, E., and Zenk, M.H. (1993). Signaling in the elicitation process is mediated through the octadecanoid pathway leading to jasmonic acid. Proc. Natl. Acad. Sci. USA **90:** 7490–7494.

Newman, J.D., and Chappell, J. (1999). Isoprenoid biosynthesis in plants: Carbon partitioning within the cytoplasmic pathway. Crit. Rev. Biochem. Mol. Biol. **34:** 95–106.

Ohnmeiss, T.E., and Baldwin, I.T. (2000). Optimal defense theory predicts the ontogeny of an induced nicotine defense. Ecology **81:** 1765–1783.

Ohnuma, S.-I., Hirooka, K., Tsuruoka, N., Yano, M., Ohto, C., Nakane, H., and Nishino, T. (1998). A pathway where polyprenyl diphosphate elongates in prenyltransferase. J. Biol. Chem. **41:** 26705–26713.

Paschold, A., Bonaventure, G., Kant, M.R., and Baldwin, I.T. (2008). Jasmonate perception regulates jasmonate biosynthesis and JA-Ile metabolism: The case of COI1 in *Nicotiana attenuata.* Plant Cell Physiol. **49:** 1165–1175.

Paschold, A., Halitschke, R., and Baldwin, I.T. (2007). Co(i)-ordinating defenses: NaCOI1 mediates herbivore-induced resistance in *Nicotiana attenuata* and reveals the role of herbivore movement in avoiding defenses. Plant J. **51:** 79–91.

Pearce, G., Moura, D.S., Stratmann, J., and Ryan, C.A. (2001). Production of multiple plant hormones from a single polyprotein precursor. Nature **411:** 817–820.

Pearce, G., Ramcharan, B., Chen, Y.-C., Barona, G., Yamagachi, Y., and Ryan, C.A. (2009). Isolation and characterization of hydroxoproline-rich glycopeptide signals in black nightshade leaves. Plant Physiol. **150:** 1422–1433.

Ren, F., and Lu, Y.-T. (2006). Overexpression of tobacco hydroxyproline-rich glycopeptide systemin precursor A gene in transgenic tobacco enhances resistance against Helicoverpa armigera larvae. Plant Sci. **171:** 286–292.

Reymond, P., Weber, H., Damond, M., and Farmer, E.E. (2000). Differential gene expression in response to mechanical wounding and insect feeding in *Arabidopsis.* Plant Cell **12:** 707–719.

Rhoades, D.F. (1979). Evolution of plant chemical defense against herbivores. In Herbivores: Their Interaction with Secondary Plant Metabolites, G. Rosenthal and D. Janzen, eds (New York: Academic Press), pp. 3–54.

Ribot, C., Zimmerli, C., Farmer, E.E., Reymond, P., and Poirier, Y. (2008). Induction of the *Arabidopsis PHO1;H10* gene by 12-oxo-phytodienoic acid but not jasmonic acid via a CORONATINE INSENSITIVE1-dependent pathway. Plant Physiol. **147:** 696-706.

Roda, A., Oldham, N.J., Svatoš, A., and Baldwin, I.T. (2003). Allometric analysis of the induced flavonols on the leaf surface of wild tobacco (*Nicotiana attenuata*). Phytochemistry **62:** 527–536.

Ryan, C.A., and Pearce, G. (2003). Systemins: A functionally defined family of peptide signals that regulate defensive genes in Solanaceae species. Proc. Natl. Acad. Sci. USA **100:** 14577–14580.

Saedler, R., and Baldwin, I.T. (2004). Virus-induced gene silencing of jasmonate-induced direct defences, nicotine and trypsin proteinase-inhibitors in Nicotiana attenuata. J. Exp. Bot. **55:** 151–157.

Sandermann, H., Jr. (1994). Higher plant metabolism of xenobiotics: the 'green liver' concept. Pharmacogenetics **4:** 225–241.

Sandermann, H., Jr., Schmitt, R., Eckey, H., and Bauknecht, T. (1991). Plant biochemistry of xenobiotics: isolation and properties of soybean O- and N-glucosyl and O- and N-malonyltransferases for chlorinated phenols and anilines. Arch. Biochem. Biophys. **287:** 341–350.

Schiffman, S.S., and Gatlin, C.A. (1993). Sweeteners - State of knowledge review. Neurosci. Biobehav. Rev. **17:** 313–345.

Schilmiller, A.L., and Howe, G.A. (2005). Systemic signaling in the wound response. Plant Biol. **8:** 369–377.

Schmidt, S., and Baldwin, I.T. (2009). Down-regulation of systemin after herbivory is associated with increased root allocation and competitive ability in *Solanum nigrum.* Oecologia **159:** 473–482.

Schwachtje, J., and Baldwin, I.T. (2008). Why does herbivore attack reconfigure primary metabolism? Plant Physiol. **146:** 845–851.

Schwachtje, J., Kutschbach, S., and Baldwin, I.T. (2008). Reverse genetics in ecological research. PLoS One **3:** e1543.

Schwachtje, J., Minchin, P.E.H., Jahnke, S., van Dongen, J., Schittko, U., and Baldwin, I.T. (2006). SNF1-related kinases allow plants to tolerate herbivory by allocating carbon to roots. Proc. Natl. Acad. Sci. USA **103:** 12935–12940.

Selmar, D., Lieberei, R., and Biehl, B. (1988). Mobilization and utilization of cyanogenic glycosides: the linustatin pathway. Plant Physiol. **86:** 711–716.

Shinozaki, Y., Tobita, T., Mizutani, M., and Matsuzaki, T. (1996). Isolation and identification of two new diterpene glycosides from *Nicotiana tabacum.* Biosci. Biotechnol. Biochem. **60:** 903–905.

Siritunga, D., and Sayre, R. (2004). Engineering cyanogen synthesis and turnover in cassava (*Manihot esculenta*). Plant Mol. Biol. **56:** 661–669.

Snook, M.E., Johnson, A.W., Severon, R.F., Teng, Q., White, R.A., Sisson, V.A., Jr., and Jackson, D.M. (1997). Hydroxygeranyllinallol glycosides from tobacco exhibit antibiosis activity in the tobacco budworm. *Heliothis virescens* (F.). J. Agric. Food Chem. **45:** 2299–2308.

Steppuhn, A., Gase, K., Krock, B., Halitschke, R., and Baldwin, I.T. (2004). Nicotine's defensive function in nature. PLoS Biol. **2:** 1074–1080.

Suzuki, H., Nakayama, T., Yonekura-Sakakibara, K., Fukui, Y., Nakamura, N., Yamaguchi, M., Tanaka, Y., Kusumi, T., and Nishino, T. (2002). cDNA cloning, heterologous expressions, and functional characterization of malonyl-coenzyme a:anthocyanidin 3-o-glucoside-6″-o-malonyltransferase from dahlia flowers. Plant Physiol. **130:** 2142–2151.

Taguchi, G., Shitchi, Y., Shirasawa, S., Yamamoto, H., and Hayashida, N. (2005). Molecular cloning, characterization, and down-regulation of an acyltransferase that catalyzes the malonylation of flavonoid and naphthol glucosides in tobacco cells. Plant J. **42:** 481–491.

Terauchi, M., Kanamori, H., Nobuso, M., Sakamoto, I., Yahara, S., Nohara, T., and Kohda, H. (1995). Analysis of acyclic diterpene glycosides in *Lycii folium*. Nat. Med. (Tokyo) **49:** 133–136.

Terauchi, M., Kanamori, H., Nobuso, M., Yahara, S., and Nohara, T. (1997a). Detection and determination of antioxidative components in *Lycium chinense.* Nat. Med. (Tokyo) **51:** 387–391.

Terauchi, M., Kanamori, H., Nobuso, M., Yahara, S., and Nohara, T. (1997b). Seasonal variation of amounts of water-soluble components in *Lycium chinense.* Nat. Med. (Tokyo) **51:** 458–460.

Terauchi, M., Kanamori, H., Nobuso, M., Yahara, S., and Nohara, T. (1998). New acyclic diterpene glycosides, lyciumoside IV–IX from *Lycium chinense* Mill. Nat. Med. (Tokyo) **52:** 167–171.

Thines, B., Katsir, L., Melotto, M., Niu, Y., Mandaokar, A., Liu, G., Nomura, K., He, S.Y., Howe, G.A., and Browse, J. (2007). JAZ repressor proteins are targets of the SCF^{COI1} complex during jasmonate signaling. Nature **448:** 661–665.

Towler, M., and Weathers, P. (2007). Evidence of artemisinin production from IPP stemming from both the mevalonate and the non-mevalonate pathways. Plant Cell Rep. **26:** 2129–2136.

Van Dam, N.M., Horn, M., Mares, M., and Baldwin, I.T. (2001). Ontogeny constrains systemic protease inhibitor response in *Nicotiana attenuata.* J. Chem. Ecol. **27:** 547–568.

Vick, B.A., and Zimmerman, D.C. (1984). Biosynthesis of jasmonic acid by several plant species. Plant Physiol. **75:** 458–461.

Wasternack, C. (2007). Jasmonates: An update on biosynthesis, signal transduction and action in plant stress response, growth and development. Ann. Bot. (Lond.) **100:** 681–697.

Wu, J., Hettenhausen, C., Meldau, S., and Baldwin, I.T. (2007). Herbivory rapidly activates MAPK signaling in attacked and unattacked leaf regions but not between leaves of *Nicotiana attenuata.* Plant Cell **19:** 1096–1122.

Xie, D.-X., Feys, B.F., James, S., Nieto-Rostro, M., and Turner, J.G. (1998). *COI1*: An *Arabidopsis* gene required for jasmonate-regulated defense and fertility. Science **280:** 1091–1093.

Yu, X.-H., Chen, M.-H., and Liu, C.-J. (2008). Nucleocytoplasmic-localized acyltransferases catalyze the malonylation of 7-O-glycosidic (iso)flavones in *Medicago truncatula.* Plant J. **55:** 382–396.

Zavala, J.A., Patankar, A., Gase, K., Hui, D., and Baldwin, I.T. (2004). Manipulation of endogenous trypsin proteinase inhibitor production in *Nicotiana attenuata* demonstrates their function as antiherbivore defenses. Plant Physiol. **134:** 1181–1190.